INFORMATION TO USERS

This manuscript has been reproduced from the microfilm master. UMI films the text directly from the original or copy submitted. Thus, some thesis and dissertation copies are in typewriter face, while others may be from any type of computer printer.

The quality of this reproduction is dependent upon the quality of the copy submitted. Broken or indistinct print, colored or poor quality illustrations and photographs, print bleedthrough, substandard margins, and improper alignment can adversely affect reproduction.

In the unlikely event that the author did not send UMI a complete manuscript and there are missing pages, these will be noted. Also, if unauthorized copyright material had to be removed, a note will indicate the deletion.

Oversize materials (e.g., maps, drawings, charts) are reproduced by sectioning the original, beginning at the upper left-hand corner and continuing from left to right in equal sections with small overlaps.

Photographs included in the original manuscript have been reproduced xerographically in this copy. Higher quality 6" x 9" black and white photographic prints are available for any photographs or illustrations appearing in this copy for an additional charge. Contact UMI directly to order.

ProQuest Information and Learning
300 North Zeeb Road, Ann Arbor, MI 48106-1346 USA
800-521-0600

Université d'Ottawa · University of Ottawa

Recovery of Surfactant-Induced Friction Reduction in a Closed Hot Water System

Joanna Bellamy

A thesis submitted to the School of Graduate Studies and Research
in partial fulfilment of the requirements for the
degree of

Master of Applied Science

in the Department of Chemical Engineering
University of Ottawa

January 2000

Table of Contents

Abstract

The potential of linear macromolecules to reduce friction in flowing fluids was first recognized by pulp industry researchers in the 1930's. Later experiments showed that polymers and surface active agents (surfactants) could achieve the same effects. Surfactants form micelles in flowing fluid and are well suited to use in closed systems because of their ability to recover after the high shear stresses encountered in pumps.

In the 1980's the use of surfactants to decrease pumping energy requirements in district heating systems was explored in Europe. FRAs are particularly attractive for district energy systems because they have long pipe runs and the associated pumping costs can be a large component of total operating costs. However, the decrease in turbulence which is beneficial in district energy distribution systems has a deleterious effect on heat transfer coefficients in shell and tube heat exchangers.

In this research project, a series of obstructing devices were designed and tested for their ability to disrupt micelles and reverse the friction reducing effect in a 3/4 inch diameter stainless steel experimental test loop. Four simple obstructing geometries were investigated: a central obstruction blocking one quarter of the flow area, a central obstruction blocking half of the flow area and two obstructions which blocked the area close to the pipe wall, blocking one half and three quarters of the flow area, respectively.

The experimental friction reducing additive was a combination of a quaternary ammonium surfactant, Ethoquad O/12, and a 3-hydroxy-2-naphthoate counterion, at concentrations of 1600 ppm and 800 ppm respectively. The obstructions were tested at three temperatures, 70, 50 and 40 Celsius and at flow rates of 3.7, 3.0 and 2.0 m/s.

The friction reducing additive was found to have two different levels of effectiveness. In two sets of test runs, one at 40°C and one at 50°C, friction reduction averaging 55% was measured, while in two other sets of runs, at 50°C and 70°C, friction reduction averaging 78% was measured. The only differences between the two FRA samples were the alcohol solvent and the mixing procedure. Friction reduction recovery distances downstream of the obstructions were found to be between 25 and 30 diameters. In two cases with particularly high shear rates (with the small hole obstruction at the highest velocity measured, 3.0 m/s) the recovery was further delayed. Obstruction geometry and flow velocity were found to have no effect on recovery distance. A simple model for recovery of friction reduction was developed to explain these observations.

Acknowledgements

I would like to extend special thanks to Dr. William Hallett for his invaluable support and guidance throughout this thesis project, and in particular during the lengthy experimental stage of the project. As well, I would like to thank Dr. Chris Snoek of the Community Energy Systems Group at the CANMET Energy Technology Centre of Natural Resources Canada, for his continuous encouragement and guidance, as well as Michael Wiggin, the technology manager of the group, for his support of the project. The advice and input of Tom Onno, a research scientist with the Community Energy Systems group, with the data acquisition systems and instrumentation, was a very valuable and much appreciated contribution to the project as was the enthusiastic participation of Randy Biggs and Mike Channing. I would like to also thank Dr. Martin Hellsten, Guy Barrette and Gerry Archambault of Akzo Nobel for supplying the friction reducing additives tested in this experiment.

Nomenclature

b	ratio of the cross sectional area of the tube to the cross sectional area of the obstruction plate, dimensionless
D	pipe diameter, m
e	height of protuberances in circular tube flow (e/D is the relative roughness), m
f	Fanning friction factor, dimensionless
$f_{solvent}$	friction factor for the pure solvent, dimensionless
f_{fra}	friction factor for the solution containing the friction reducing additive, dimensionless
f_{limit}	maximum limiting friction factor (surfactant systems), dimensionless
$K_{mismatch}$	constant used to represent the pressure loss due to misalignment at the obstruction plate junction, dimensionless
K_{offset}	constant used to verify corrections applied to pressure tap measurements, dimensionless
K	kD/V, a rate constant for the formation of micelles, dimensionless
k	a rate constant for the formation of micelles, dimensionless
L	length along the test section, m
m	mass flow rate of fluid, kg/s
P	pressure, inches H_2O
Re	Reynolds Number, dimensionless
t_I	induction time for formation of the micelle shear-induced state
t_S	plateau time for the formation of the shear-induced state
u	fluid velocity, m/s
u^+	dimensionless velocity = u/u_τ
u_τ	shear velocity = $(\tau_w/\rho)^{1/2}$, m/s
V	characteristic velocity for the shear layer downstream of an obstruction, m/s
V_O	velocity in the unobstructed pipe
V_S	velocity at the obstruction plate
y^+	dimensionless distance from the wall

Greek Symbols

η	percent friction reduction or FRA efficiency, dimensionless
η_∞	maximum friction reduction or limiting FRA efficiency, dimensionless
μ	fluid viscosity, g/(cm s)
τ	shear stress, dyne/cm^2
τ_w	wall shear stress, dyne/cm^2
ρ	density, kg/m^3

Acronyms

FRA	friction reducing additive
RTD	resistance temperature detector
SIS	shear induced state

List of Tables

List of Figures

1.0 Introduction

The use of surfactant-based friction reducing additives (FRAs) to reduce pressure losses in closed hot and cold water distribution systems has potentially significant economic and environmental benefits. FRAs are particularly attractive for district energy systems because they have long pipe runs and high pumping costs. Surfactant-based additives form rod-like micelles in flowing fluid which act to suppress the formation of turbulent eddies in the fluid and reduce fluid friction. Frictional loss reductions in excess of 80% have been measured in straight segments of piping: this can translate into pressure loss reductions of 60-70% in district energy systems.

Decreases in pressure losses can result in reductions in operating costs and energy consumption by reducing the energy required for pumping. Alternatively, the additives can be used to increase the capacity of existing district energy distribution networks by increasing the volume of fluid which can be pumped through the system with the same pumping energy input. Both of these benefits increase the economic viability of district energy systems.

It is hoped that friction reducing additives may have a role in increasing the implementation of district energy systems in Canada. By allowing communities to make use of waste or low grade sources of energy for heating and cooling in place of fossil fuels, district energy systems can decrease energy consumption and reduce the release of

products of combustion (including CO_2, NO_x, SO_2 and particulates).

Barriers to the implementation of friction reducing additives include concerns about environmental impact in the event of leakage, compatibility with chemicals used to protect against corrosion, and most significantly, decreased heat transfer in heat exchangers where convection is the primary mode of heat transfer. Chemists are addressing environmental concerns by developing additives which are biodegradable and of low toxicity to marine organisms. At Akzo-Nobel Laboratories in Sweden, researchers have developed new groups of additives including alkyl betaines with alkyl benzene sulphonates. This new FRA was successfully tested in a 5.6 km distribution system in Herning, Denmark, achieving an overall friction reduction of 70%, pumping energy savings of 50% and energy savings equivalent to $1.45 million US over a one-year period.

Pipe friction reduction is usually quantified in terms of the Fanning friction factor (Bird, Stewart and Lightfoot, 1960):

$$f = \frac{2\tau}{\rho u^2} = \frac{D}{2\rho u^2}\frac{dP}{dL} \qquad (1.1)$$

The percent friction or drag reduction is equal to the difference between the friction factor of the solvent and that of the solution containing the additive at identical conditions divided by the friction factor of the solvent:

$$\eta = \frac{f_{solvent} - f_{fra}}{f_{solvent}} \cdot 100\% \qquad (1.2)$$

The following Moody diagram shows the well-established Hagen-Poiseuille and Prandtl-Karman relationships which describe friction as a function of Reynolds number in laminar and turbulent pipe flow. The points on the graph show the typical behaviour of an FRA solution: it suppresses turbulence, so that the friction factor is reduced nearly to the value one would get by extending the laminar flow curve.

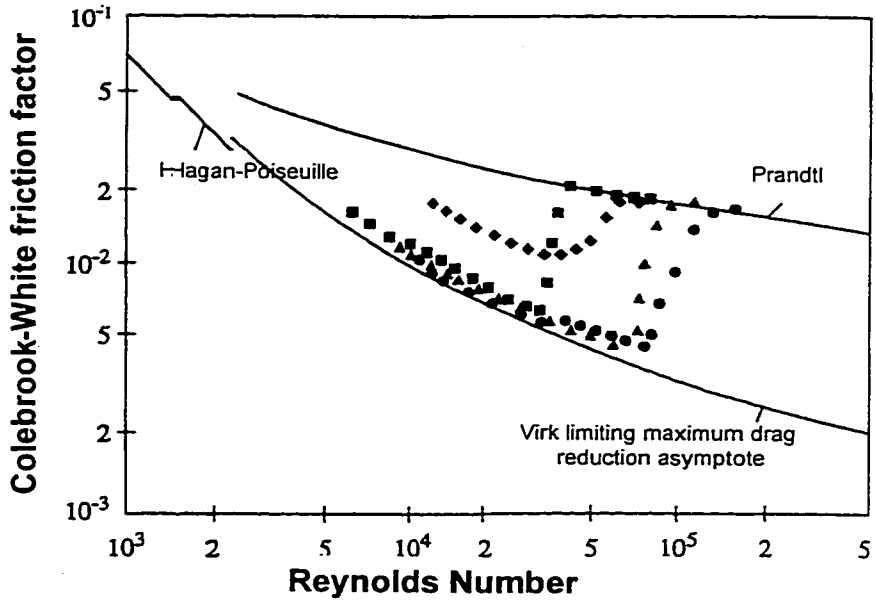

Figure 1.1 - Friction factor vs. Reynolds Number
(After De Groot and Kievet, 1996)

The Hagen-Poiseuille law, which describes laminar flow in tubes, is (Bird, Stewart and Lightfoot, 1960):

$$f = \frac{16}{\mathrm{Re}} \qquad (1.3)$$

and the Prandtl resistance law, which describes turbulent flow in smooth tubes, is:

$$\frac{1}{\sqrt{f}} = 4.0 \log_{10}\left(\mathrm{Re}\sqrt{f}\right) - 0.40 \qquad (1.4)$$

Also indicated on the graph is the empirically-derived Virk limiting maximum drag reduction asymptote, which indicates the extent to which friction factors can be reduced in systems containing polymer drag reducing additives. The data points indicate the existence of a critical Reynolds number or critical shear beyond which the FRA micelle structures break down and friction reduction ceases. The actual value of critical shear rate is specific to the particular additive as well as being a function of the concentration of the additive and the temperature of the solution.

While decreased turbulence is beneficial in distribution piping, it is a disadvantage in heat exchangers where it leads to depressed heat transfer coefficients. Heat transfer in shell-and-tube heat exchangers has been shown to be reduced by 75-95% when friction reducing additives are used. However, the literature shows that heat transfer coefficients can be temporarily restored to higher levels by applying shear stresses that are high enough to cause micellar structures to break down. The effect is reversible and once the shear stress is removed the micelles 'recover', i.e. re-form their turbulence damping structures.

1.1 Objective

The goal of this research project was to investigate micellar disruption and recovery as a step in assessing the possibility of increasing heat transfer in FRA flows for district heating. A series of obstructing devices were designed and tested for their ability to restore friction losses in pipes to normal levels by creating sufficient shear to reverse the friction reducing effect. Pressures were measured across and downstream of these obstructing devices in order to draw conclusions about recovery distances, the relative effectiveness of various geometries, and the effect of velocity and temperature on FRA recovery. In the following chapters, the literature on FRAs is surveyed, the experimental apparatus is described, and the results presented.

2.0 Literature Search

2.1 General

The first reports of friction reducing phenomena were made by Forrest working in the pulp industry in the 1930s, who noted that the flow of solutions containing pulp fibres continued to be laminar, even at high flow rates (Forrest, 1931). At the First International Rheological Conference in 1948 Toms reported that when small amounts of linear macromolecules were added to flowing fluids, the wall shear stress of the fluid was significantly reduced (Toms, 1949). Another observation was that the specific energy required to pump the solution in turbulent flow was lower than for the pure solvent. Toms measured friction reduction of up to 50% in a dilute solution (0.25% by weight) of polymethyl methacrylate in monochlorobenzene. This report gave rise to the name 'Toms Effect' to describe friction reduction. Mysels observed the same effect in 1949 while working with anionic surfactants (aluminum soaps) used as thickening agents in gasoline (as referenced in Shenoy, 1984 and Hoyt, 1972).

A number of additives have been demonstrated as having friction reducing properties. These include suspensions of solid particles such as fibres, polymers such as guar gum and polyethylene oxide, biological additives such as sea water slime, and surfactants.

2.2 Polymers

A number of researchers have investigated the friction reducing behaviour of polymer solutions. Early work in this area was reported by Dodge and Metzner (1959), Shaver and Merrill (1959), Savins (1967) and Fabula et al. (1963). Dodge and Metzner (1959) and Shaver and Merrill (1959) all noted that non-Newtonian fluids (i.e. solutions with a variable viscosity which depends on the rate of shearing) had low friction factors and documented low friction in solutions of carboxymethylcellulose. As well, Shaver and Merrill showed from dye streaks that turbulence was lower in flowing solutions of the polymer than in the pure solvent.

Fabula et al. (1963) were the first to identify polyethylene oxide as one of the most effective friction reducing additives - only a few parts per million of the polymer were required to reduce friction coefficients substantially. Hoyt reported drag reduction of 40% for a 0.5 ppm solution of polyethylene oxide and 75% drag reduction at a 25 ppm concentration in a 1.02 cm diameter tube at a Reynolds number of 10^5. He also noted that any macromolecule that has a linear structure and a sufficient molecular weight (greater than 50,000 g/mole) could be expected to cause friction reduction (Hoyt, 1972). However, Cho and Hartnett (1982) reported that the drag reducing effect with a particular polymer additive at a fixed concentration may not be quantitatively reproducible, since friction reduction depends upon solvent chemistry, polymer degradation and tube diameter.

In 1971 Virk proposed an empirically-derived relationship to describe the limiting maximum drag reduction which can be attained based on data from polymer systems:

$$\frac{1}{\sqrt{f}} = 19\log(\mathrm{Re}\sqrt{f}) - 32.4 \qquad (2.1)$$

This corresponds to a friction reduction of approximately 80%.

A characteristic of drag reducing polymer systems is the requirement of a threshold shear stress for friction reduction, which is associated with the force needed to untangle and straighten the molecules. This characteristic has been documented by a number of researchers, some of whom have derived relationships to predict the threshold stress. Virk (1971) proposed a relationship in which the onset of drag reduction occurs at a constant value of the product of the dimension of the macromolecule and K_D, a wave number characteristic of turbulent flow. Fabula proposed a similar but different relationship (as referenced in Hoyt, 1972).

In addition to a threshold shear stress required for the onset of friction reduction, a critical shear stress exists for polymer solutions beyond which chemical bonds in the molecules are broken and friction reduction ceases. Matthys (1991) demonstrated this effect in a system of AP-273 Separan in tap water. He showed that by intentionally degrading the solution by strong mechanical stirring the drag reducing effect was decreased and heat transfer

coefficients increased. Pollert and Sellin (1989) reported on the breakdown of polymers and reversal of drag reduction by shearing in a pump as well as the effect of severe elongational strain in pipe entrances at high flow rates in causing this effect. This degradation is irreversible. Polymer solutions have been found to degrade with time even without strong shear, and this gradual loss of friction reduction has been a major drawback to their application in practical systems.

Developing or entrance lengths of up to 100 diameters (for hydrodynamic entrance effects) and 600 diameters (for thermal entrance effects) have been reported for polymer solutions (Matthys, 1991), while typical entrance lengths for Newtonian fluids in turbulent flow are of the order of 20 diameters. Matthys noted that the eddy diffusivity for momentum is much greater than that for heat for friction reducing fluids. He also noted that entrance length for polymers increases as the Reynolds number increases. Cho and Hartnett (1982) reported mass, momentum and heat transfer entry lengths of 35, 100 and 500 diameters, respectively.

Friction reducing additives impact on the velocity profiles of fluids in turbulent flow. Hoyt (1972) noted that friction reducing polymers create profiles that are much flatter than for water, while nonviscoelastic non-Newtonian fluids (fluids which do not exhibit friction reducing properties) and Newtonian fluids have the same velocity profiles in turbulent flow.

A detailed discussion on the changes in profile appears in Hoyt (1972). The turbulent velocity profile in a pipe can be expressed in terms of u^+, a dimensionless velocity equal to u/u_τ (u_τ is the shear velocity, equal to $(\tau_w/\rho)^{1/2}$) and y^+, the dimensionless distance from the wall,

$$u^+ = \frac{u}{u_\tau} \qquad (2.2)$$

$$y^+ = \frac{yu_\tau}{\nu} \qquad (2.3)$$

The log law, valid for $y^+>30$ for Newtonian fluids in turbulent flow, is

$$u^+ = A \ln y^+ + B \qquad (2.4)$$

where A= 2.5 and B = 5.5 for Newtonian fluids

Hoyt demonstrated that the addition of friction reducing polymers leads to a thickened laminar sublayer, evidence that the action of polymers is in an elastic sublayer or 'buffer zone', indicated in Figure 2.1 below. He proposed that a constant, ΔB, be added to equation 2.4 above to reflect the increase in the local velocity ratio, u^+, when friction reducing polymers are present. A similar model was presented by Matthys and Sabersky (1982), who showed that the offset ΔB is characteristic for a given FRA and concentration.

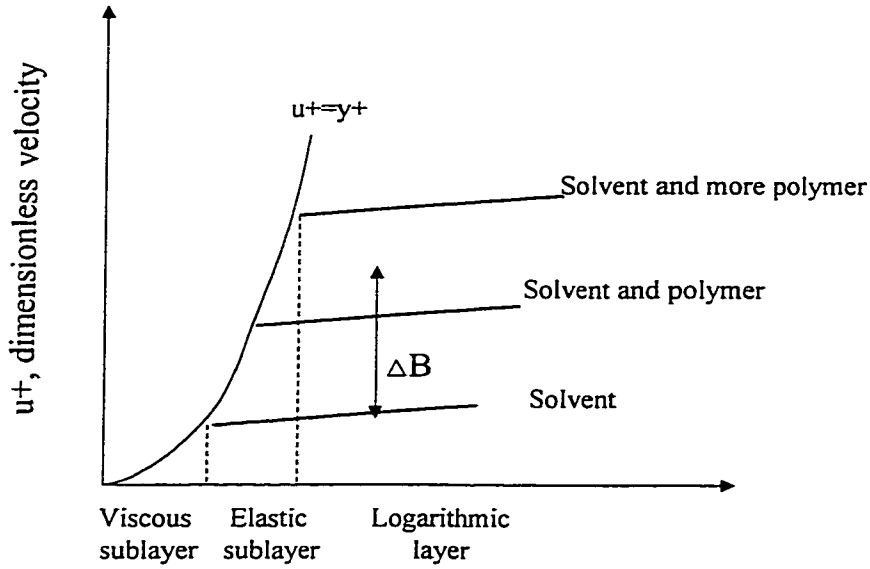

Figure 2.1 - Velocity profiles for fluids in turbulent flow

As mentioned above, friction reduction is not always quantitatively reproducible and changes in pipe diameter will change the friction coefficients (Matthys, 1991). Matthys has developed a model for polymers to predict the friction coefficient for a given diameter based on experimental data obtained for a different diameter which uses the velocity profile model outlined above. Cho and Hartnett (1982) reported that the drag reduction effect with polyethylene oxide can be strongly affected by the chemistry of the water in which the polymer is dissolved. They also reported variations in friction reduction from one batch of polymer to another, possibly due to differences in average polymer length.

2.3 Surfactants

Another class of additives are surfactants, or surface active agents. These are amphiphilic molecules which have a hydrophilic component and a hydrocarbon chain. The additives associate to form "micelles" (agglomerations of molecules) under certain conditions. They require higher dosages than polymers but are virtually immune to mechanical degradation and are therefore much more attractive for long term use in practical systems.

Friction reduction equal to or in excess of that predicted by Virk's limiting maximum drag reduction asymptote for polymer systems has been measured in surfactant systems. Zakin et al. (1996) have proposed the following relationship for the limit (derived from data for surfactant systems) which corresponds to a maximum friction reduction in excess of 80%

$$f_{limit} = \frac{1.26}{4} Re^{-0.55} \qquad (2.5)$$

Cationic, anionic, non-ionic and zwitterionic surfactants have been investigated for their friction reducing potential as well as their suitability in district energy applications. Anionic surfactants have the disadvantage that they react with the calcium and magnesium ions commonly present in tap water to form insoluble salts. Non-ionic surfactants are thought to have good potential for development since they are chemically stable and are unlikely to precipitate out of solution in the presence of contaminants. Zwitterionic surfactants contain headgroups which have cationic and anionic areas, but

similarly are overall electrically neutral, which renders them environmentally more benign.

Cationic surfactants have been most successfully applied in district energy applications. Table 2.1 below shows a family of n-alkyl quaternary ammonium chloride salts developed by Hoechst AG in Germany in the 1980s. The surfactants are used at concentrations of 500 to 1000 ppm in district heating systems and are always added together with a counterion, usually 3-hydroxy-2-naphthoate or salicylate, which is added in concentrations that are typically in the range of half of the surfactant concentration. The additives are effective at temperatures of 30-150°C. The role of the counterion is to reduce the electrostatic repulsion between the charged surfactant headgroups and to allow the headgroups to approach each other more readily.

Table 2.1 - Cationic friction reducing additives developed for district heating applications by Hoechst AG

Trade name	Quaternary ammonium cation	Counterions
Habon	n=16	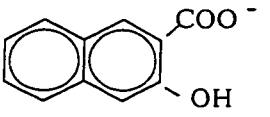 3-hydroxy-2-naphthoate
Obon	n=18	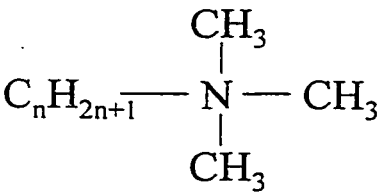
Dobon	n=22	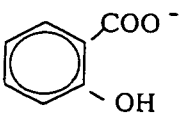 Salicylate

Table 2.2 gives the structures of new families of additives which are being developed for district energy applications and which have reduced environmental impacts.

Table 2.2 - New families of environmentally benign FRAs
(R=n-alkyl radical)

Fatty acid amide ethoxylates	R CONH $(C_2H_4O)_nH$	- fast biodegradation - only effect at 0-40°C - low toxicity - requires high dosage
N-alkyl betaines and alkyl benzene sulphonates	R N^+ $(CH_3)_2$ CH_2COO^- and $C_{12}H_{25}$-C_6H_4 $SO_3^-Na^+$	- fast biodegradation - effective over large temp. intervals - moderate toxicity - moderate dosage
N-alkyl sarcosinates	R N^+ H_2 CH_2 COO^-	- fast biodegradation - only high temp applications - low dosage - expensive to produce

2.3.1 Micelle Formation with Surfactants

When added to water, surfactant molecules orient themselves to form an aggregate in which the headgroups are exposed and the hydrocarbon tails are inside the aggregate. The driving force for this association is the minimization of the Gibbs Free Energy of the

system. The mixing of two species will occur if the mutually attractive free energy is less than the self-attractive energies. The mixing of water with hydrocarbons is not favoured relative to the mixing of water with itself. This self-attraction is large due to hydrogen bonding. This drives micelle formation (Ohlendorf et al., 1986).

The aggregation of surfactants in water can take the form of spherical or cylindrical micelles or lamella (Figure 2.2), depending on the concentration of the surfactant and the nature and size of the hydrophilic headgroup (steric and electrostatic considerations). One of the parameters of significance is the ratio of the cross-sectional area of the headgroup to the cross sectional area of the hydrocarbon tail (steric considerations). If this ratio is 1:1, a lamellar structure is favoured. If the ratio is 2:1 a rod-like structure is favoured, while a ratio of 3:1 promotes the formation of a globular structure (Ohlendorf et al., 1986). The formation of rod-like micelles is required for friction reduction to occur (Fankhänel, 1987).

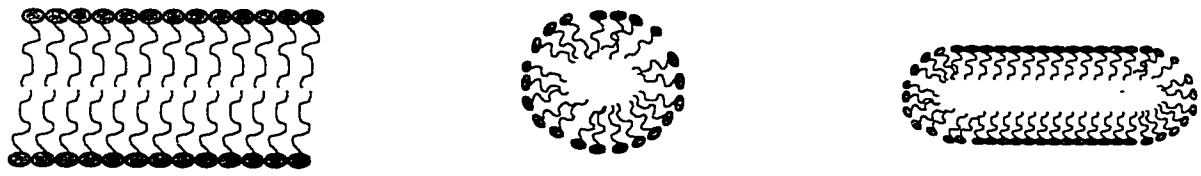

Figure 2.2 - Aggregation structures of surfactant molecules

A transition from the monomer state to rod-like micelles occurs when a characteristic surfactant concentration, the critical micellar concentration or CMC, is exceeded. Figure 2.3 below shows a critical micellar concentration curve for a typical surfactant and indicates the temperature dependence of the CMC. The Krafft point is the intersection of the solubility curve of the monomer and the CMC curve. At temperatures above the Krafft point micelles will form if the dosage exceeds the CMC (Weinspach, 1996).

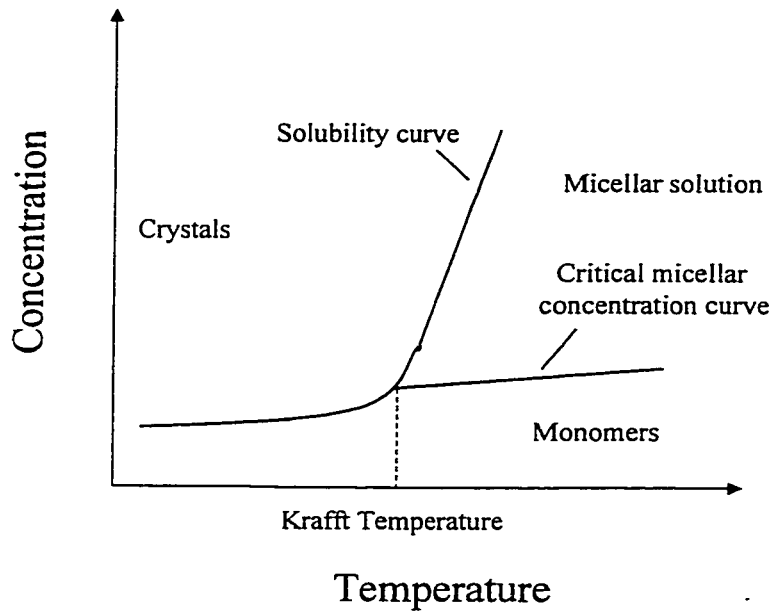

Figure 2.3 - Critical micellar concentration curve

The action of friction-reducing surfactant solutions is not only dependent on the formation of rod-like micelles in the solution, however. To obtain friction reduction a 'shear-induced -state' (SIS) must exist in which the micelles are completely aligned in the

direction of flow (see Figure 2.4 below). Evidence of this alignment was obtained by Bewersdorff and colleagues in flow birefringence studies (Rehage et al., 1986). A minimum shear rate is required to induce the SIS. The transition is accompanied by a sudden increase in the viscosity of the solution (Hu and Matthys, 1995). It is believed that the micelles form more complex secondary structures during this transition. Two mechanisms have been proposed, one in which the rods join together to form longer flexible structures that act like linear macromolecules, and a second in which the SIS is associated with the formation of an ordered lattice of individual rods (Figure 2.4) due to cooperative electrostatic interaction (Bewersdorff and Ohlendorf, 1988). An excessively high level of shear - well above that required to create the SIS - will cause the SIS to break apart again, but (unlike polymer FRAs) a return to lower shear will allow the SIS to reform.

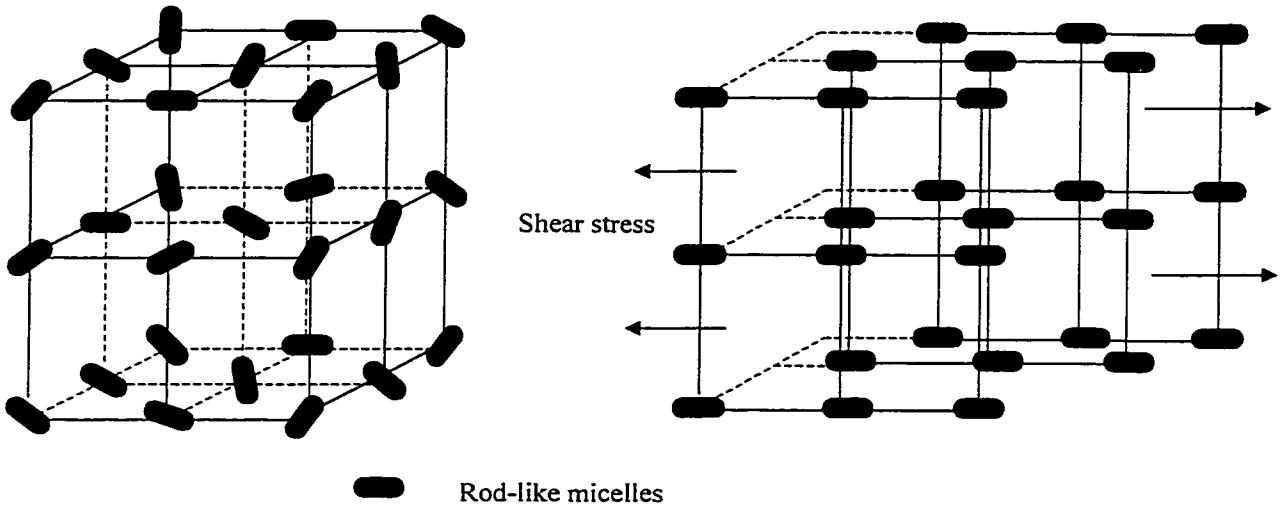

Figure 2.4 - Shear-Induced-State (SIS) of rod-like micelles
(after De Groot and Kievit, 1996)

Hu and Matthys (1995) reported on experiments in which measurements of solution first normal stress differences were used to investigate the shear-induced state in addition to viscosity and flow birefringence measurements in a 5/5 mM solution of tris (2-hydroxyethyl tallowalkyl ammonium acetate) and sodium salicylate. They noted that an induction period is required for the first formation of the SIS, but after break-up of the SIS through excessive shear no further induction period is required to re-form the SIS . They theorized that this is due to the fact that there are residual aggregates of micelles present after shearing which do not exist originally. Recovery of the SIS after shear terminated was shown to have a double exponential decay process and relaxation time was shown to decrease as shear rate increased. Gasljevic and Matthys (1997) reported much longer recovery lengths after shearing a solution of the same surfactant and counterion through a wire mesh plug. This may be because the shearing was much greater, destroying the residual micelles as well.

2.3.2 Surfactant Solutions in Pipe Flow

Equation 2.1 appears plotted in Figure 2.5 below, together with the Prandtl curve which gives the friction factor for Newtonian fluids in fully turbulent flow, and the Hagen-Poiseuille curve, which gives the friction factor for Newtonian fluids in laminar flow.

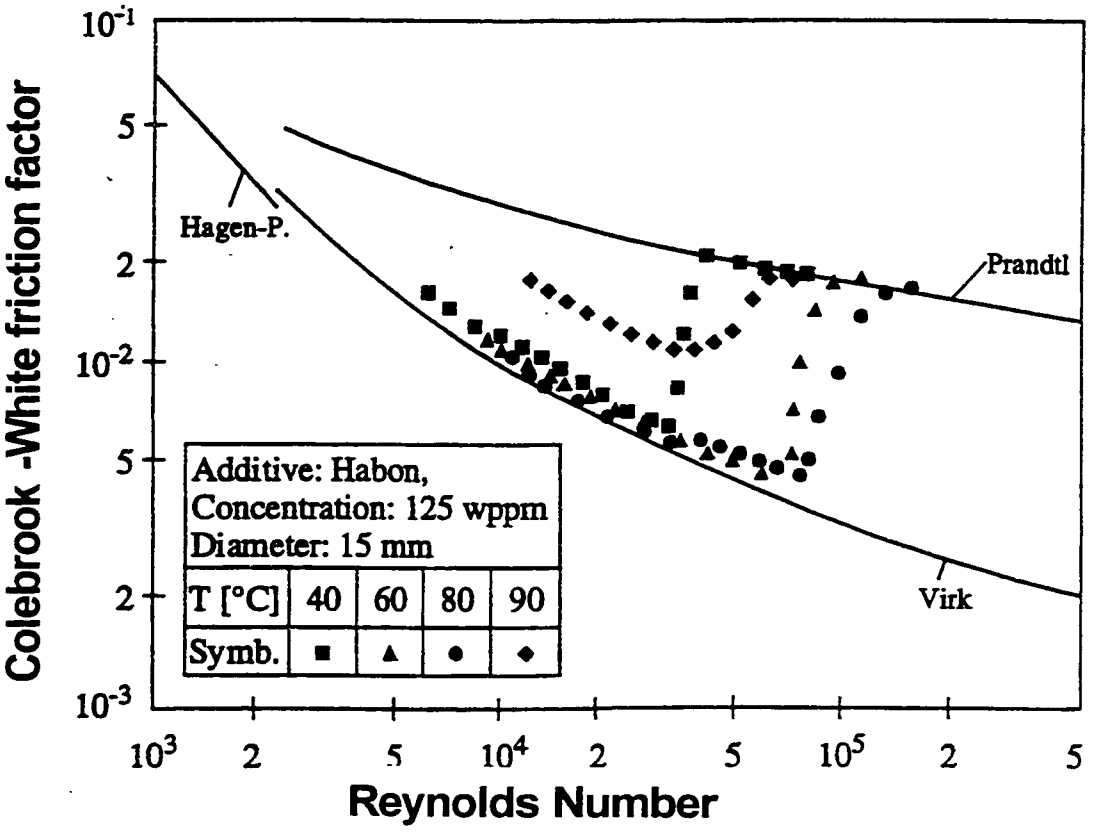

Figure 2.5 - Friction factor vs. Reynolds Number (Moody Diagram)
(after De Groot and Kievit, 1996)

The data indicate behaviours characteristic of all surfactant solutions. First, a critical shear stress exists beyond which the friction reducing effect disappears. This is reversible in surfactant systems but not in polymer systems: if the shear is reduced below the critical level the SIS will re-form and the friction reduction is re-instated. Bewersdorff et al. (1989) reported that this loss of friction reduction is accompanied by a loss of alignment of micelles (i.e. a breakdown of the SIS) although the rod-like micelles themselves were

still found to be present. Second, the friction reduction disappears at a critical temperature.

Ohlendorf et al. (1986) reported this effect and noted that friction reduction ceased at critical temperatures despite the fact, again, that electric birefringence studies indicated the presence of rod-like micelles. It has been postulated that the critical temperature is due to the breakdown of the secondary structures, and that this is due to a decrease in micellar size at higher temperatures (Fankhänel et. al., 1989). Ohlendorf et al. (1986) have theorized that the upper temperature limit exists because beyond this the time constant for the formation and disintegration of rod-like micelles becomes so small that no secondary structures build up. Third, the upper temperature limit is dependent on the micelle concentration - it is higher for a higher micelle concentration.

2.3.3 Mechanism

When the potential of surfactants as friction reducing additives was first being explored, White (as referenced in Shenoy, 1984) claimed that the threshold stress for friction reduction that exists for polymer friction reducing solutions did not exist in the cetyl trimethyl ammonium bromide solutions he was working with. However, numerous authors since then (Hu and Matthys, 1995, Gasljevic and Matthys, 1991, Fankhänel et al. 1987, Ohlendorf et. al, 1986) have shown that a minimum shear rate is necessary to set up the SIS and produce drag reduction, albeit a much lower shear than with polymers.

Shenoy (1984) has noted that high velocity gradients are required to lengthen polymer molecules before friction reduction occurs and that surfactants require lower velocity gradients to achieve the shear-induced state required for friction reduction. Clearly there are a number of morphological differences between surfactant and polymer systems which influence the mechanism of friction reduction in each.

Myska and Zakin (1996) have identified five characteristics which distinguish polymer systems from surfactant systems, including the response to shear degrading conditions, the limiting maximum friction reduction asymptotes, tube diameter effects, viscosity-shear rate relationships, and velocity profiles. They concluded that there are likely to be differences in microstructures and friction reducing mechanisms which account for these characteristics. They observed that when surfactant solutions are degraded by shear the effect is reversible and the original amount of friction reduction is always recovered. Polymers do not demonstrate this self-healing effect, as high stresses permanently break chemical bonds in the molecules. As discussed above and indicated in equations 2.1 and 2.5, the maximum achievable friction reduction is greater for surfactant solutions than for polymer solutions.

The diameter effect, in which friction reduction decreases with increasing pipe size, has been described by a number of authors for both surfactant and polymer systems, including Matthys and Sabersky (1982) and Sellin and Ollis (1983). Moderate success was reported in developing models to predict frictional coefficients as a function of pipe diameter.

Surfactant solutions decrease in viscosity with increasing shear at low shear rates but demonstrate increased viscosities at higher shear rates, due to the formation of a shear-induced structure. The viscosity continues to increase with the length of time of shearing until it reaches an asymptotic value (Hu and Matthys, 1995). Polymer solutions used in friction reducing applications, on the other hand, demonstrate shear-thinning. Surfactant solutions also show steeper velocity profiles (Myska and Zakin, 1996).

Myska and Zakin (1996) concluded that the differences in the associative forces of the two types of additives, the "secondary molecular forces" which hold together micelles and the SIS in surfactant solutions and the covalent bonds in polymers, as well as the differences in the structures themselves, may explain these differences in behaviour.

Bewersdorff and Ohlendorf (1988) have proposed two theories about where in the flow the damping of turbulence takes place in surfactant systems. One theory is that the buildup of ordered structures in the core region of the pipe damps large scale turbulence. The second theory is that structures of aligned rods damp the turbulence in the near wall boundary layer of the flow.

Fankhänel et al. (1987) described the mechanism of drag-reducing surfactants as follows: "With sufficient shear stress near the wall surfactants build up a supermicellar structure, which leads to an increase in viscosity and to an extension of the elastic sublayer (buffer layer)....the development and movement (rotation) of dissipative vortices is suppressed

strongly." They suggest that the elastic structure of the SIS temporarily absorbs the energy of forming turbulent eddies. When the SIS reexpands the energy is then out of phase. The result is that fluid turbulence is suppressed. Cho and Hartnett (1982) suggested a similar mechanism in polymer systems, theorizing that the turbulent kinetic energy of the fluid is temporarily converted into elastic strain energy of the polymer.

2.4 Heat Transfer

One of the most significant barriers to the widespread use of friction reducing additives is the decrease in heat transfer which accompanies the decrease in turbulence. This impacts significantly on overall heat transfer coefficients when convection is the primary mode of heat transfer. For example, in shell-and-tube heat exchangers decreases in heat transfer coefficients in excess of 90% have been measured (Weinspach, 1996). The impact is less significant in heat exchangers whose structures induce turbulence, such as helical tube heat exchangers (45-70% reduction in heat transfer coefficient) and plate heat exchangers (45-70% reduction) (Gasljevic et al., 1993).

A number of researchers, including Gasljevic and Matthys (1994 and 1997), Young (1994) and Blais et al. (1996), have shown that heat transfer coefficients can be temporarily restored to higher levels by shearing the flow to levels in excess of the critical shear stress and reversibly disrupting the micelles.

Young (1994) showed that a partially closed valve could be used to increase depressed heat transfer coefficients in a shell and tube heat exchanger by 50%. The pressure penalty of achieving this was quite significant compared to the pressure savings in the rest of the compact cooling system, however. Friction reduction in compact (building) systems is typically smaller than in district energy systems with long pipe runs because of the breakdown of micelles by elbows, and contractions. However, these are not significant sources of shearing and recovery is usually rapid. Gasljevic and Matthys (1997) demonstrated recovery of heat transfer after an elbow of 60 diameters. They have also shown (Gasljevic and Matthys,1992) that friction reduction downstream of a centrifugal pump is recovered within 150 diameters even at Reynolds numbers as high as 150,000, indicating small degradation effects.

Gasljevic and Matthys (1994 and 1997) have investigated the use of critical shear to deliberately break down micellar structures and recover heat transfer in a solution of 2300 ppm Ethoquad T13 and 2000 ppm sodium salicylate in deionized water at temperatures of 10-40°C. They examined friction factors and heat transfer coefficients downstream of a conical entry and a series of wire mesh plugs. With the conical entry, they observed that the friction and heat transfer reduction could be significantly reversed, but that the effect was short-lived, with complete recovery of heat transfer and friction reduction after approximately 20 diameters. With the plug entries, recovery also occurred within 100

diameters except at the highest velocities examined (6.9 m/s), for which the depressed friction reduction and increased heat transfer effects lasted about twice as long. However, the pressure loss of the wire mesh plug was very high (equivalent to 2000 diameters). They also observed that, contrary to the evidence for polymer systems, developing temperature and velocity profiles in surfactant systems appeared to be coupled, but that development of heat transfer appeared identical for surfactant and polymer solutions.

Entrance effects are observed in surfactant systems, as in polymer systems. Gasljevic and Matthys (1997) reported entrance lengths of 300 diameters for both hydrodynamic and thermal development.

Blais et al. (1996) carried out an experiment in which a series of static mixers were inserted into the flow, and were able to completely reverse the reduced heat transfer. However, the pressure loss across the mixers was roughly 2-3 times greater than the pressure drop across the heat exchanger.

2.5 District Heating Applications

Benefits of the use of friction reducing additives in district energy systems are reductions in pressure losses and pumping energy requirements, the potential to increase the heating or cooling load connected to the system by increasing the volume flow rate of fluid in the

system (with the same pumping energy input), and the potential to decrease distribution pipe sizes in new systems for the same reason which results in lower capital costs for the system.

Cationic surfactant additives have been successfully demonstrated in district heating systems in Volkingen, Germany (International Energy Agency,1990), Herning, Denmark (Hammer, 1998), and Kladno-Krocehlavy, Czech Republic (Pollert et al., 1996). In the Volkingen demonstration, which took place in 1988 in a 1.2 km distribution pipeline connecting a community to a combined heat and power plant, pressure loss reductions of 70% were measured. The additive used in the system was Dobon at a concentration of 1150 ppm.

A recent demonstration with new environmentally benign additives developed by Akzo-Nobel in the 5.6 km transmission line connecting the Herning district heating system to a combined heat and power plant nearby resulted in 70% savings in the energy required for pumping. The problem of decreased heat transfer coefficients was overcome by oversizing the heat exchangers in the system.

In the demonstration in the Kladno-Krocehlavy system pumping energy requirements were reduced by 41% by adding 450 ppm of Habon. No reduction in overall heat transfer coefficients was measured at all. Researchers believed that this was due either to very hot

tube walls or due to the presence of scale on the tube walls which was already providing a significant resistance to heat transfer. Laboratory testing with the same additive indicated a reduction in the overall heat transfer coefficient in a plate fin heat exchanger of 25%.

Young (1994) showed that heat transfer coefficients could be completed restored to original levels by throttling an inlet valve to a heat exchanger in a building cooling system in Halifax. The FRA had reduced heat transfer coefficients in the chiller by 55%. The pressure 'penalty' of using the valve to cause micellar breakdown however was very high (6.5 psi, equivalent to more that a third of the pressure drop through the entire system).

2.6 Conclusion

A review of the literature has indicated that micellar 'recovery' in surfactant systems is not completely understood. Efforts that have been made to reverse friction reduction by creating shear stresses high enough to cause micellar breakdown have been accompanied by significant pressure losses. Gasljevic and Matthys (1997) reported pressure losses equivalent to 2000 diameters for wire mesh plug obstructions while Blais et al. reported pressure losses equivalent to 2-3 times that of the heat exchanger itself when static mixers were used to recover heat transfer in a plate heat exchanger.

The goal of this research project, therefore, was to evaluate whether obstructions with moderate pressure losses can effectively disrupt micelles and to evaluate how long the

effects last. Other goals were to assess where in the flow shearing was most effective, and to draw conclusions about the effect of temperature and velocity on micellar recovery. From this, it was hoped that conclusions could be drawn about the feasibility of disrupting heat exchanger flows to improve heat transfer.

3.0 Methodology

The purpose of the experiments was to determine the effects of different shear-generating obstructions on pressure losses in pipe flows with FRAs. Obstructions were placed at the beginning of the pipe test section, and measurements of pressure loss along the pipe were made both in FRA flows and in pure water. This chapter details the experimental techniques and data reduction methods used.

3.1 Experimental Design

A test loop was constructed to measure the pressure drop across and downstream of a set of obstruction plates, described below. The design of the loop allowed the insertion of each plate in turn by opening a gasketed connection at the entry to the test section. A schematic diagram of the test loop appears in Figure 3.1.

The nominal diameter of the tubing in the test loop and test section was 3/4 inch (actual internal diameter of 17.05 mm ± 0.1 mm, with a wall thickness of 0.89 mm). This diameter was selected as a 'compromise' between the smaller diameters of piping typical in building systems (in the range of 1/4-1/2 inch) and the larger diameters characteristic of district heating systems (in the range of 2 to 6 inches) as well as diameters typical in tube and shell heat exchangers. Because of inaccuracies in scale-up with FRA solutions, there was a desire to carry out tests with pipe diameters as close as possible to those in actual

systems.

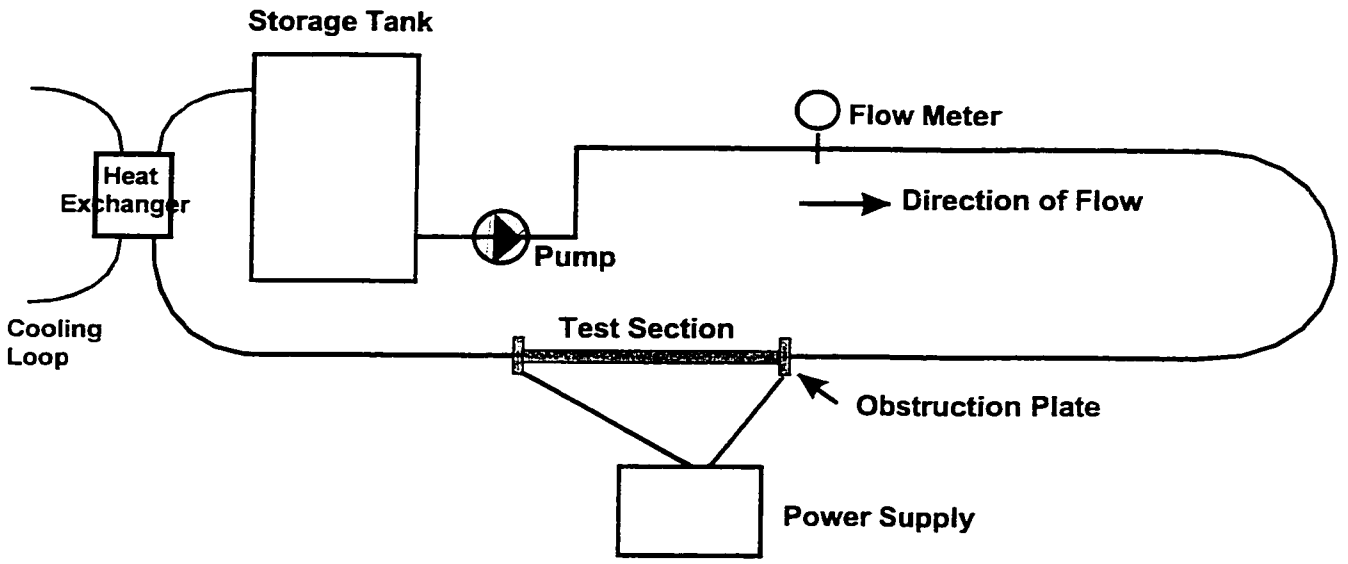

Figure 3.1 - Schematic of experimental test loop

Another restriction with respect to diameter related to the heat transfer studies planned for later in the research program and the goal of producing a measurable temperature gradient of at least 10°C along the test section. Thin-walled Inconel tubing, of higher resistivity than stainless steel and producing higher heat fluxes, was selected for the test section for this reason also.

Pressure tap holes 2mm in diameter were drilled in the Inconel test section tubing at twenty locations 5 to 150 diameters downstream of the point of insertion of the obstruction plates (Figure 3.2). (Literature has shown that hydrodynamic recovery distances of 100 diameters are typical for surfactants at the velocities in this experiment

(Gasljevic and Matthys, 1997)). Great care was taken to avoid the formation of metal burrs around the holes by inserting a metal cylinder into the tubing below the tap during drilling. After drilling, the holes were inspected for burrs to the extent possible and sanded both internally and externally. Pressure tap fittings were machined from plastic disks and were attached as two semi-circular halves, bolted together. Tiny polybutylene o-rings were used to create a seal between the pipe surface and the pressure tap fitting (Figure 3.3).

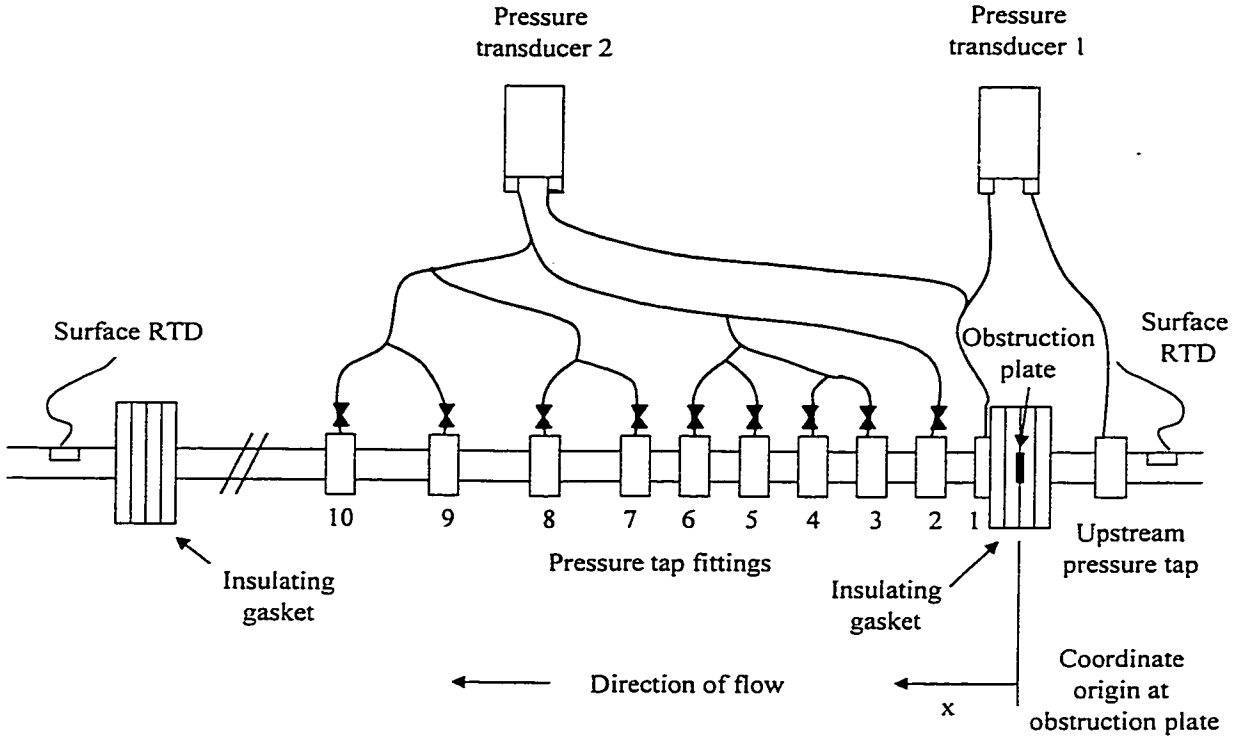

Figure 3.2 - Schematic of experimental test section

Pressure was measured across the obstruction plate by two taps connected via clear plastic tubing to a pressure transducer, transducer 1 in Figure 3.2, calibrated to measure pressure

differences of up to 100 inches of water (25.3 kPa). Nine additional taps were connected to a second pressure transducer, transducer 2, calibrated to measure pressure differences of up to 40 inches of water (10 kPa). Each tap could be read in turn by opening small valves fitted to the plastic tubing. The remaining ten taps were capped and ready to use in the event that measurement of the pressure drop at different locations proved important later in the experiment. The use of two transducers allowed the measurement of pressure without sacrificing resolution, which is a function of the full range of the transducer. Manufacturers' specifications give the accuracy of both transducers as ±0.5% of full range.

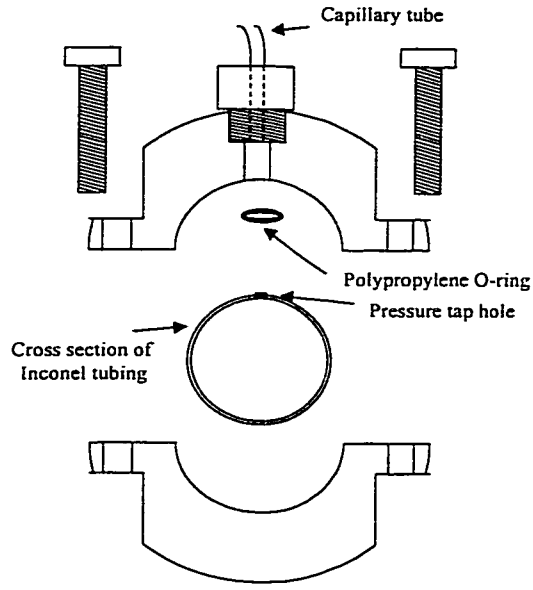

Figure 3.3 - Pressure tap fitting

Four obstruction plates of simple geometry shown schematically in Figure 3.4 were designed to create shearing at different locations in the cross-section of the flow. Two,

the bigger and smaller disk, obstructed the flow at the centre, creating a wake effect, and blocking respectively ½ and ¼ of the cross-sectional area of the tube. The other two, a bigger and a smaller hole, blocked ½ and ¾ of the flow area respectively, creating a jet in the flow. The plates were held by Teflon gaskets machined to hold them in place and align them with the test section tubing (Figure 3.5). A "blank" obstruction, with the same internal diameter as the test section, was also prepared, to allow tests in a straight undisturbed tube.

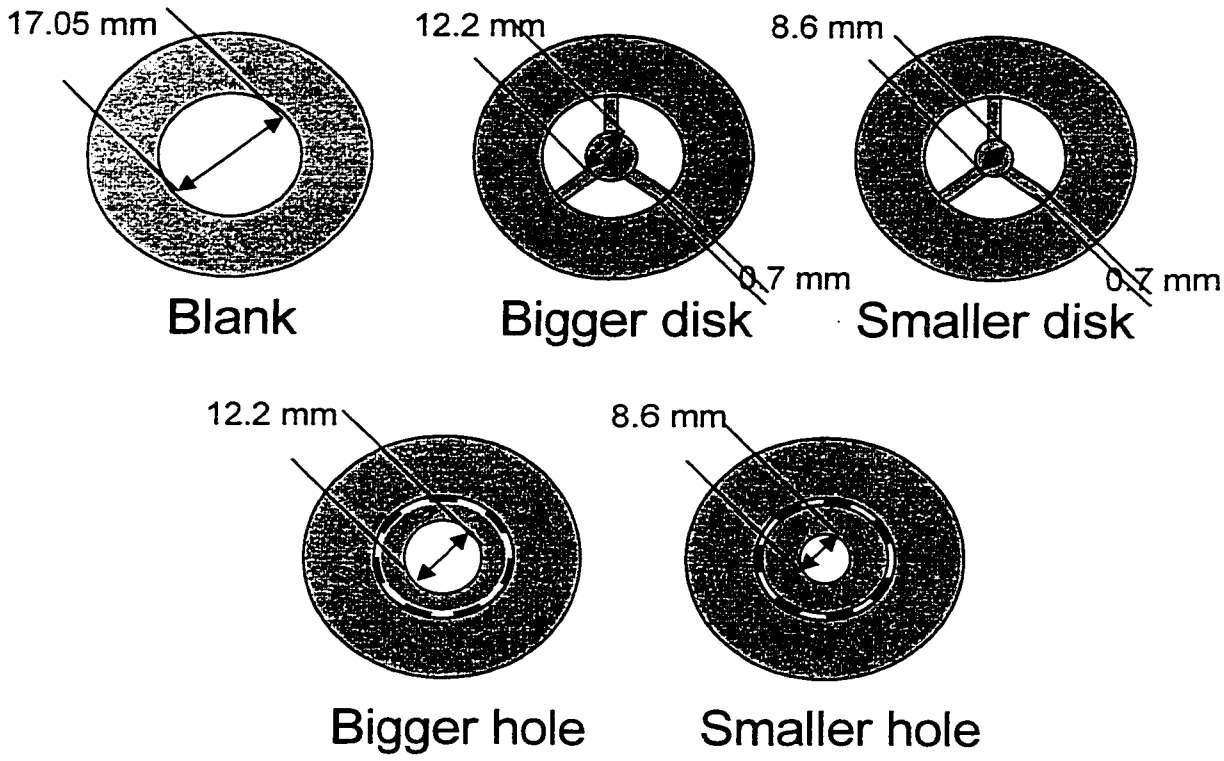

Figure 3.4 - Obstruction plates (dotted line indicates tubing diameter)

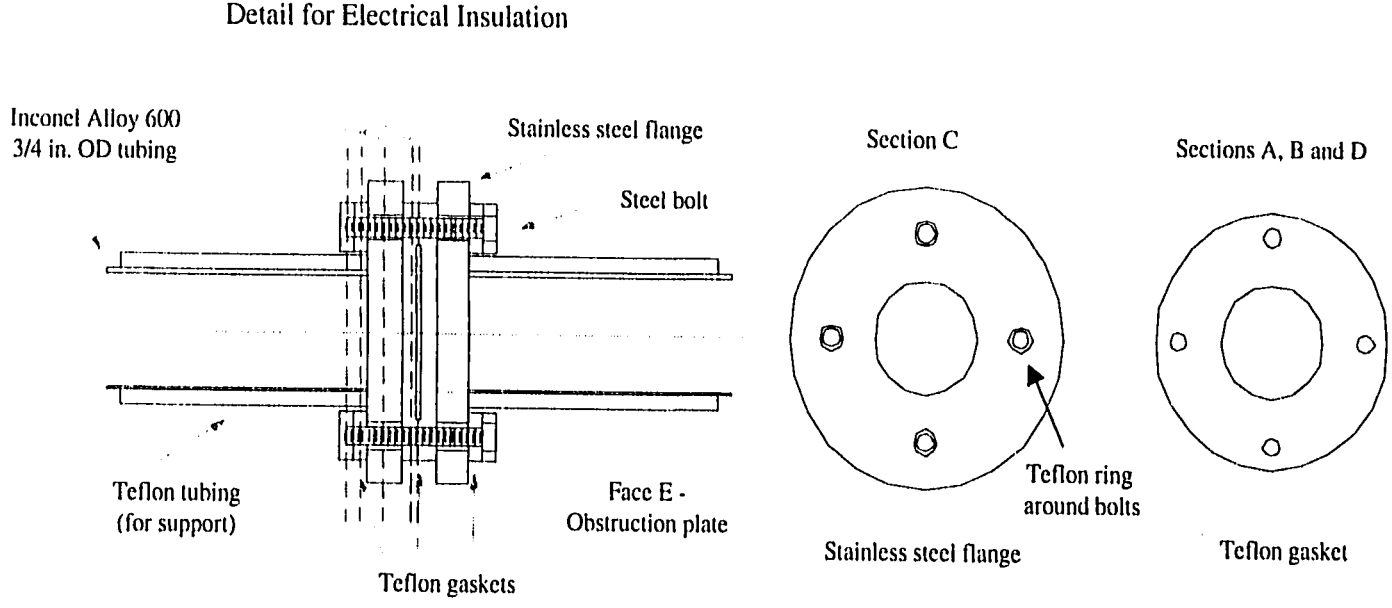

Figure 3.5 - Teflon gasket connection

All of the components in the loop were stainless steel or, in the case of the test section, Inconel, to eliminate the possibility of rusting within the test loop. Products of corrosion have been reported to interfere with the performance of friction reducing additives (Young, 1995). The use of copper in the test loop has also been avoided because of reports of amines reacting with copper (Young,1995).

The test section was located downstream of a 5 m straight segment of piping to ensure fully developed flow at the entry to the test section; this is particularly important in view of the fact that the lengths required for flow development are longer with FRAs than for water (Gasljevic and Matthys, 1997). It was also considered desirable to leave a long length of pipe after the pump, in case of breakup of micelle aggregates by the pump rotor. The test section was insulated electrically from the rest of the stainless steel loop by two Teflon gasket connections (Figure 3.5) and connected to a 25 kW (50 VDC, 500 A maximum output) power supply which served as the heater for the system. These limits for the output of the power supply were chosen with safety considerations in mind. The connection of the test section to the power supply allowed application of constant heat fluxes down the length of the test section and will be important for measurement of heat transfer coefficients in future experiments.

A storage tank was added to maintain a large thermal mass and to minimize temperature fluctuations, with supply taken from the bottom and returned to the top of the tank to ensure good mixing within the tank. The test loop and storage tank were insulated with

foam rubber insulation. The test loop was instrumented with probe and surface RTDs to measure inlet and outlet temperatures to the test section. The experimental temperatures drifted downward slightly during the course of the experiments. The maximum drift was at the highest temperatures where the temperature fell from 72 to 68 °C over the course of the 4 hours of measurement.

The flow rate was measured using a Chlorius magnetic flow meter with a maximum range of 3.6 m^3/h. Literature has shown that the presence of friction reducing additives will not adversely affect the accuracy of this type of flow meter, while FRAs may affect the performance of turbine, impeller and vortex-shedding flow meters (Groth et al., 1994).

Calibration of the flow meter indicated that it was accurate to within ± 0.5%. A low flow high head stainless steel centrifugal pump was selected, capable of producing a pressure head of 210 kPa.

Measurements of pressure, temperature, and flow rate were recorded on a FLUKE data acquisition system. Several seconds were required after opening each tap valve for the pressure reading to stabilize. A number of readings of pressure (every 2 seconds for 30-50 seconds) were taken for the taps connected to transducer 2 in order to ensure that the asymptotic pressure was reached for each tap. In some cases, the tap holes may have become partially blocked due to slippage of the polybutylene o-rings. These taps had higher time constants and required a greater length of reading time for the asymptotic

pressure to be reached.

3.2 Experimental Method

Pressure differences were measured and recorded across the four obstruction plates and one blank and at locations downstream for three flow rates, 3.7, 3 and 2 m/s (corresponding to Reynolds numbers of approximately 110,000, 90,000 and 60,000 based on the viscosity of pure water at 50°C) and three temperatures of interest, 70, 50 and 40°C, two of them, 70 and 50°C, characteristic of supply and return temperatures respectively in 'low temperature' district heating systems. Tests were carried out at these conditions for water, in order to establish a reference, and then for solutions containing FRAs. Table 3.1 below gives the matrix of experimental conditions examined. Because of the high pressure loss created by the small hole obstruction plate, the maximum velocity was limited in that case to 3 m/s.

3.3 Surfactant Properties

The initial intention was to carry out tests using a sample of new environmentally benign alkyl benzene and benzene sulphonate additives provided by Akzo-Nobel (Sweden). However, when added to the test system in the concentrations recommended, these additives did not produce any drag reduction at all. Researchers at Akzo suggested that this could have been due to the presence of dissolved calcium and magnesium ions in the

Table 3.1 - Experimental test matrix

FRA_1 = Ethoquad 0/12 H surfactant (isopropyl alcohol solvent), 3-hydroxy-2-naphthoate counterion

FRA_2 = Ethoquad 0/12 PG surfactant (1,2-propanediol solvent), 3-hydroxy-2-naphthoate counterion

Test run	Temperature and nominal velocities	Blank	Bigger disk	Smaller disk	Bigger hole	Smaller hole
1	40°C - 3.7 m/s	FRA_1	FRA_1	FRA_1	FRA_1	
	3 m/s	FRA_1	FRA_1	FRA_1	FRA_1	FRA_1
	2 m/s	FRA_1	FRA_1	FRA_1	FRA_1	FRA_1
2	50°C - 3.7 m/s	FRA_1	FRA_1	FRA_1	FRA_1	
	3 m/s	FRA_1	FRA_1	FRA_1	FRA_1	FRA_1
	2 m/s	FRA_1	FRA_1	FRA_1	FRA_1	FRA_1
3	50°C - 3.7 m/s	FRA_2	FRA_2	FRA_2	FRA_2	
	3 m/s	FRA_2	FRA_2	FRA_2	FRA_2	FRA_2
	2 m/s	FRA_2	FRA_2	FRA_2	FRA_2	FRA_2
4	70°C - 3.7 m/s	FRA_2	FRA_2	FRA_2	FRA_2	
	3 m/s	FRA_2	FRA_2	FRA_2	FRA_2	FRA_2
	2 m/s	FRA_2	FRA_2	FRA_2	FRA_2	FRA_2

water. However, deionized water was used in the system and a chelating agent was added as well to the system to bind any calcium and magnesium which could have built up on components and redissolved. Testing with a second sample provided by Akzo produced the same results.

As an alternative, a surfactant belonging to the N-alkyl quaternary ammonium family, Ethoquad O/12, and the counterion 3-hydroxy-2 naphthoate were chosen. Researchers at Saint Mary's University had measured friction reduction of 57% when this surfactant and counterion were added to test systems at 70°C at concentrations of 2.5 mM (corresponding to 1000 and 500 ppm for the surfactant and counterion, respectively) (Young 1995). In this experiment the surfactant concentration was 1600 ppm and the counterion concentration was 800 ppm. The chemical structure of the additives is given in Figure 3.6.

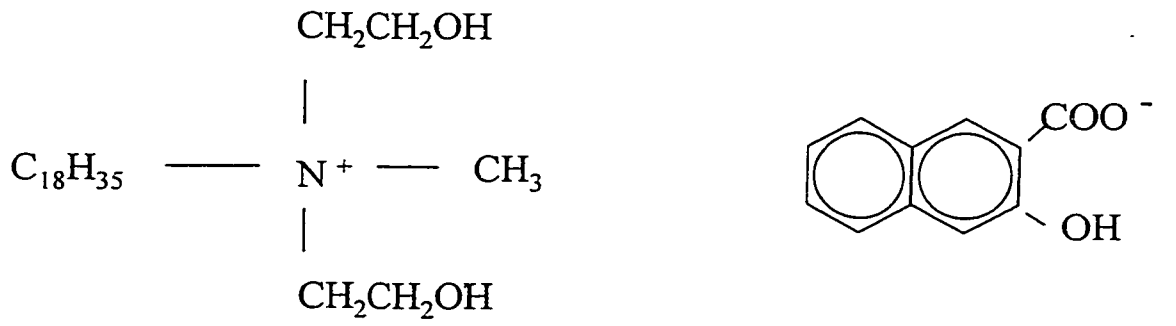

Ethoquad 0/12

3-hydroxy-2-naphthoate

Figure 3.6 - Chemical structure of experimental surfactant and counterion

An initial surfactant sample, Ethoquad 0/12 H, was obtained from Akzo-Nobel (U.S) in December 1998. This first surfactant preparation was 75% by mass surfactant and 25% by mass isopropyl alcohol, an alcohol solvent. Results of tests with this surfactant are reported as FRA_1. In the second sample, received in October 1999, the alcohol solvent was replaced with 1,2- propanediol. Results of tests with the second surfactant are reported as FRA_2. Material Safety Data Sheets for the two surfactant samples are given in Appendix C.

3.4 Data Reduction Procedure

3.4.1 Pressure Tap Corrections

Despite the care taken to eliminate burrs from the pressure taps, the measured pressures show consistent and repeatable deviations, which are clearly due to pressure tap problems and must be corrected for. Figure 3.7 shows cumulative pressure measurements as a function of axial distance for test run 1 (FRA_1 at 40°C) for water and the FRA solution with a "blank" obstruction (i.e. open tube) at the three test velocities. Data obtained at pressure tap 10 were excluded from the analysis as the measurements at this location were not repeatable. The data for water are consistent with the Colebrook relationship, giving a straight line relationship between pressure and distance. A line of best fit, as determined by least squares fitting, is also shown. It is apparent that there are deviations from the line of best fit which repeat. For example, readings at pressure tap 7 are consistently lower

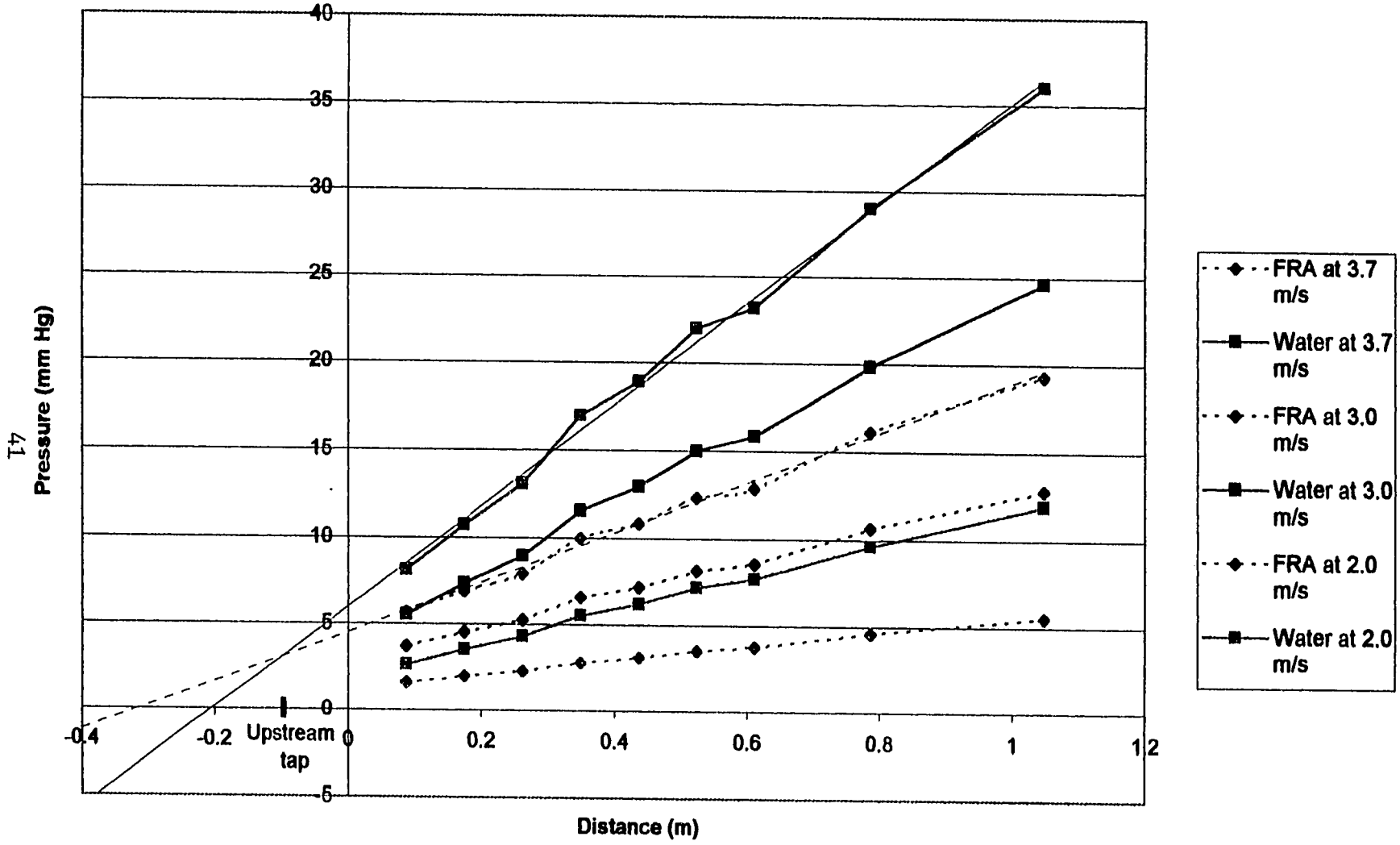

Figure 3.7 - Pressure vs. distance for FRA1 and for water at 50C with blank obstruction

than the best fit line. It is believed that these deviations are due to some irregularity at the tap, such as a burr, and not to random error. To test this, these effects can be expressed as pressure coefficients.

$$K_{offset} = \frac{\Delta P_{offset}}{\rho u^2 / 2} \qquad (3.1)$$

When this was done, the values of K_{offset} for a given tap were found to be constant regardless of flow conditions. It is therefore legitimate to use these offsets to correct all the data. A matrix of 'offset' values was developed for each test run for both water and FRA cases by subtracting experimental readings for the blank case from the line of best fit. These offsets were then applied as corrections to the pressure measurements for the obstruction plates.

Also of note is the fact that the line of best fit does not pass through the location of the upstream tap. It is believed that this is due to misalignment, inconsistent diameters or out-of-round errors at the upstream junction which create a pressure loss. Despite careful efforts to machine the blank obstruction and Teflon gaskets to obtain a completely smooth junction, the following measurements taken with a vernier caliper indicate that the internal cross section in the junction region is not always consistent. As well, the 'cradle' in the Teflon gasket which held the obstruction plate was not a perfect fit and may have allowed for some misalignment of the blank obstruction.

Table 3.2 - Internal diameters at obstruction plate junction

Component	Horizontal diameter (mm)	Vertical diameter (mm)
Upstream Teflon gasket	17.32	17.31
Blank obstruction plate	17.22	17.22
Downstream Teflon gasket	17.17	17.20
Test section	16.95	17.03

As a result of this 'mismatch', the pressure profile along the tubing can be represented as shown in Figure 3.8.

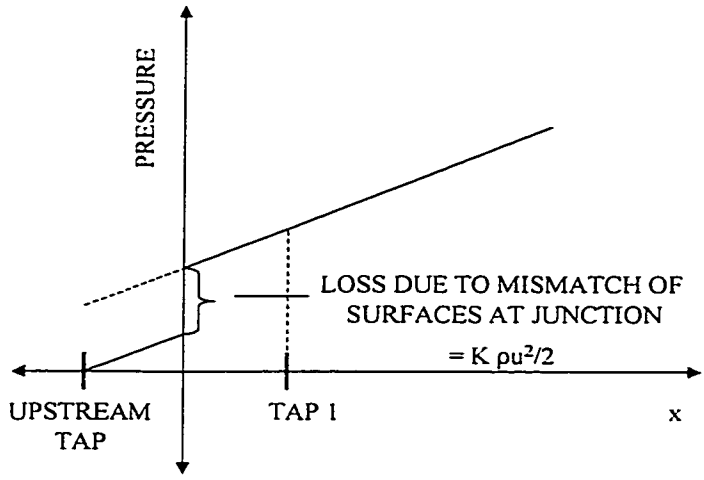

Figure 3.8 - Schematic representation of pressure loss vs. axial distance at the obstruction junction with blank obstruction plate in place

The loss due to the mismatch at the blank obstruction plate can be described by the following relationship, where the K term represents the loss due to the misalignment at the junction, $K_{mismatch}$, and the f term assumes that the straight pipe loss is the same as that

given by the best fit line downstream. It is expected that $K_{mismatch}$ should be the same for all velocities.

$$\Delta P_{U1} = \left(f \frac{L_{U1}}{D} + K_{mismatch} \right) \frac{\rho u^2}{2} \qquad (3.2)$$

where the subscript "U1" means from the upstream tap to tap 1. $K_{mismatch}$ is tabulated for each experimental test run in Table 3.3 below and the consistency is apparent.

Table 3.3 - $K_{mismatch}$ values

Test run	Temperature and velocities	$K_{mismatch}$ for water (dimensionless)	$K_{mismatch}$ for FRA solution (dimensionless)
1 - FRA_1	40°C - 3.7 m/s	0.467/ρ	0.449/ρ
	3 m/s	0.468/ρ	0.436/ρ
	2 m/s	0.515/ρ	0.400/ρ
2 - FRA_1	50°C - 3.7 m/s	0.462/ρ	0.461/ρ
	3 m/s	0.474/ρ	0.455/ρ
	2 m/s	0.495/ρ	0.460/ρ
3- FRA_2	50°C - 3.7 m/s	0.462/ρ	0.316/ρ
	3 m/s	0.474/ρ	0.305/ρ
	2 m/s	0.495/ρ	0.304/ρ
4-FRA_2	70°C - 3.7 m/s	0.658/ρ	0.458/ρ
	3 m/s	0.640/ρ	0.441/ρ
	2 m/s	0.635/ρ	0.602/ρ

This loss was subtracted from the pressure difference between the upstream and tap 1 in order to get the correct value of friction factor between these points in runs with a "blank" obstruction plate.

In runs with obstructions, a second correction had to be applied in addition to the pressure tap offset corrections. The need for Teflon insulators at the inlet made it impossible to measure the pressure right at the obstruction plate; instead, the pressure runs as shown in Figure 3.9. In order to calculate f between the plate and the first pressure tap, it is necessary to find the pressure at the upstream face of the plate. This is done by subtracting the pressure loss in the tube between the upstream tap and the plate; f here is assumed identical to that from the best fit line in the "blank" run. Unfortunately, there is no reliable way to determine the pressure at the downstream face of the plate, so that the corrected pressure difference will include the loss of the plate itself which could be a significant proportion of the total pressure drop. As a result, the first value of f (i.e. between the plate and tap 1) will be overestimated; the drag reduction at this point will be underestimated, because it is expected that the very high shear at the plate will completely eliminate the FRA effect for the obstruction itself.

One could try to extrapolate the measured pressures back to find the pressure at the downstream face. However, this would be inaccurate because the flow is developing here, and the points follow a curve of unknown shape in the developing region.

Gasljevic and Matthys (1 994) suggest that pressure tap errors may occur due to the viscoelastic nature of FRA solutions. They took steps to minimize this by reaming pressure hole in their test loop and honing the inside of the test loop. They point out, however, that pressure tap errors will cancel out for identical taps and differential pressure measurements. The pressure offsets in this experiment were evidently not due to viscoelastic effects, as the deviations were consistent in water and FRA solutions.

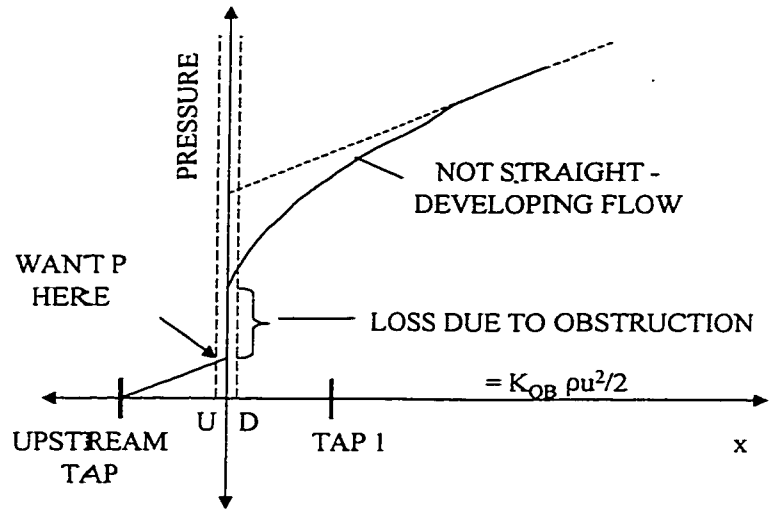

Figure 3.9 - Schematic representation of pressure loss vs. axial distance at the obstruction junction with obstruction plates in place

3.4.2. Calculation of Friction Reduction

The FRA data were compared with water data for each obstruction plate at each test velocity and temperature in order to establish the percent friction reduction. The friction factors were calculated from the equation:

$$f = \frac{D}{2\rho u^2}\frac{dP}{dL} = \frac{D}{2\rho u^2}\frac{\left(P_{tapN} - P_{tapN-1}\right)}{\left(L_{tapN} - L_{tapN-1}\right)} \quad \text{for N=2-10} \quad (3.3)$$

The per cent drag reduction was then calculated from:

$$\eta = \frac{f_{solvent} - f_{fra}}{f_{solvent}} \cdot 100\% \qquad (3.4)$$

Percent drag reduction was plotted as a function of the locations halfway between taps and linear regression was carried out to develop a curve of best fit for the data. Sample calculations are presented in Appendix A and error calculations appear in Appendix B. Percent error in friction factor calculations was calculated to be approximately 3%, and in friction reduction (FRA effectiveness) calculations, approximately 5%.

4.0 Results and Discussion

4.1 Friction Factors for Pure Water

Friction factors were calculated for each of the axial distance intervals from the 'corrected' pressure data for both water and FRA solutions for all experimental conditions. Friction factors calculated for the blank (open tube) with water were compared with values predicted by the Colebrook equation for turbulent flow:

$$\frac{1}{\sqrt{f}} = -1.72 \ln\left(\frac{e/D}{3.7} + \frac{1.255}{\mathrm{Re}\sqrt{f}}\right) \qquad (4.1)$$

where for drawn tubing e = 0.0015 mm, or e/D = 0.0001 (Perry and Green, 1984). Table 4.1 shows a comparison of these values. There is close agreement between the experimental and predicted values: the maximum deviation is 2.7%.

Table 4.1 - Friction factors for water in turbulent flow (open tube)

Test conditions	Velocity	$f_{experimental}$	$f_{Colebrook}$	% error
40°C	3.65 m/s	0.0048	0.0048	0.8
	3.00 m/s	0.0049	0.0049	-1.1
	2.00 m/s	0.0053	0.0054	-1.3
50°C	3.65 m/s	0.0047	0.0046	1.7
	3.00 m/s	0.0049	0.0048	2.3
	2.00 m/s	0.0052	0.0052	0.2
70°C	3.65 m/s	0.0045	0.0044	2.7
	3.00 m/s	0.0046	0.0045	1.3
	2.00 m/s	0.0049	0.0049	0.1

4.2 Friction Reduction Measurements

Sample plots of Fanning friction factors vs. axial distance for the bigger hole obstruction plate appear in Figures 4.1 (FRA_1 at 50°C) and 4.2 (FRA_2 at 50°C). It is evident that the friction factors are significantly lower for the FRA solutions than for water. Similar plots were obtained for all plates, and were used to calculate friction reduction for each axial distance interval.

Figures 4.3 to 4.14 show percent friction reduction plotted against axial distance downstream of the four obstruction plates and the blank obstruction for all four test runs and three velocities: FRA_1 at 40°C and 50°C (Figures 4.3 to 4.8) and FRA_2 at 50°C and 70°C (Figures 4.9 to 4.14). Most figures indicate recovery lengths of the order of 25-30 diameters. It can be seen from the figures that percent friction reduction for the various obstructions tends asymptotically towards a maximum, equal to that for the "blank" case. Table 4.2 gives these maxima for the different runs.

4.2.1 Maximum Friction Reduction

Of particular note is that the same surfactant and counterion combination added to the test system at the same concentrations produced very different results in terms of maximum friction reduction (51-59% with FRA_1 and 76-81% with FRA_2). The friction reduction produced with FRA_1 is consistent with values reported by Young (1995) in

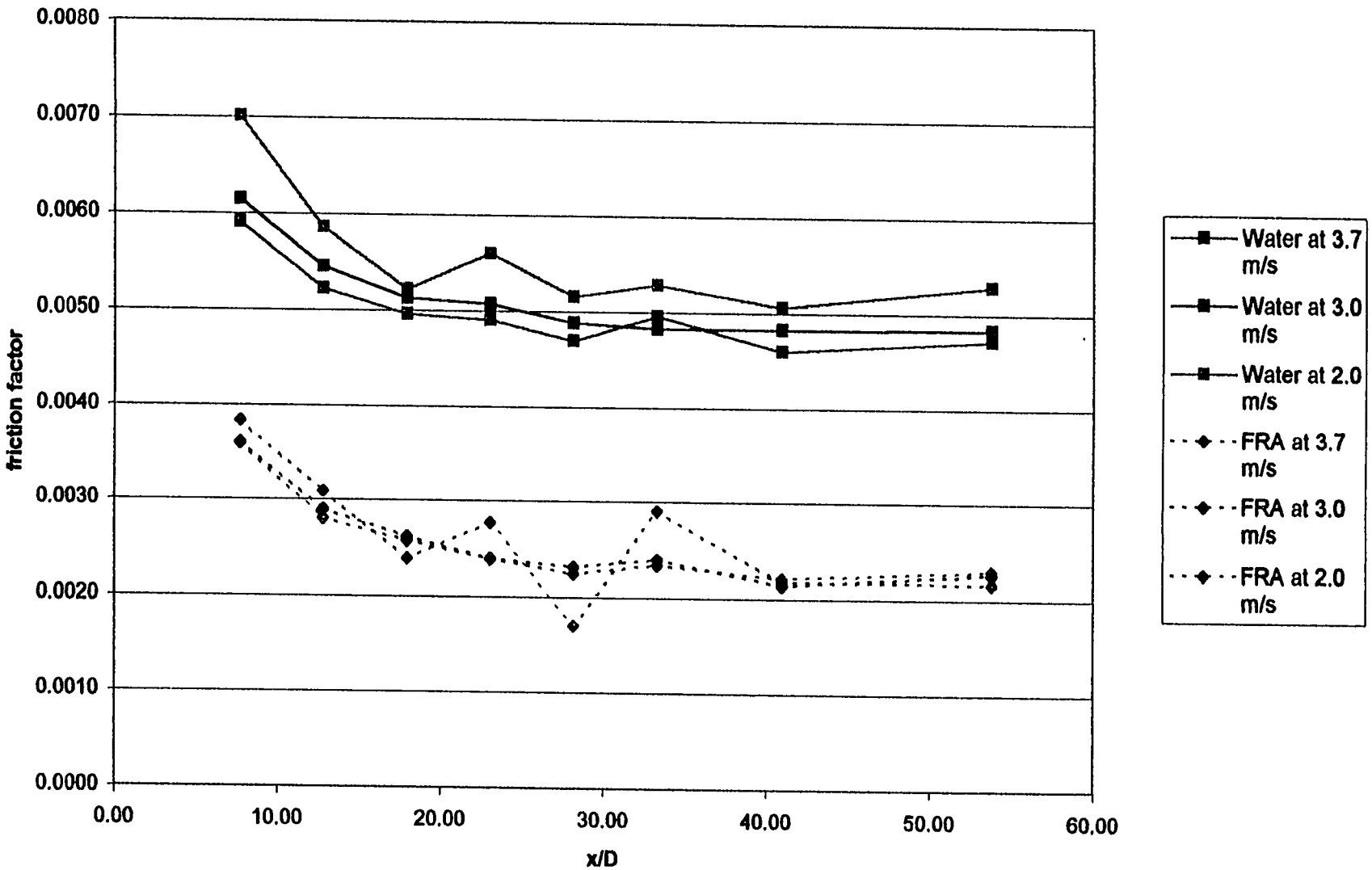

Figure 4.1 - Friction factor vs. x/D for FRA_1 with bigger hole obstruction at 50C

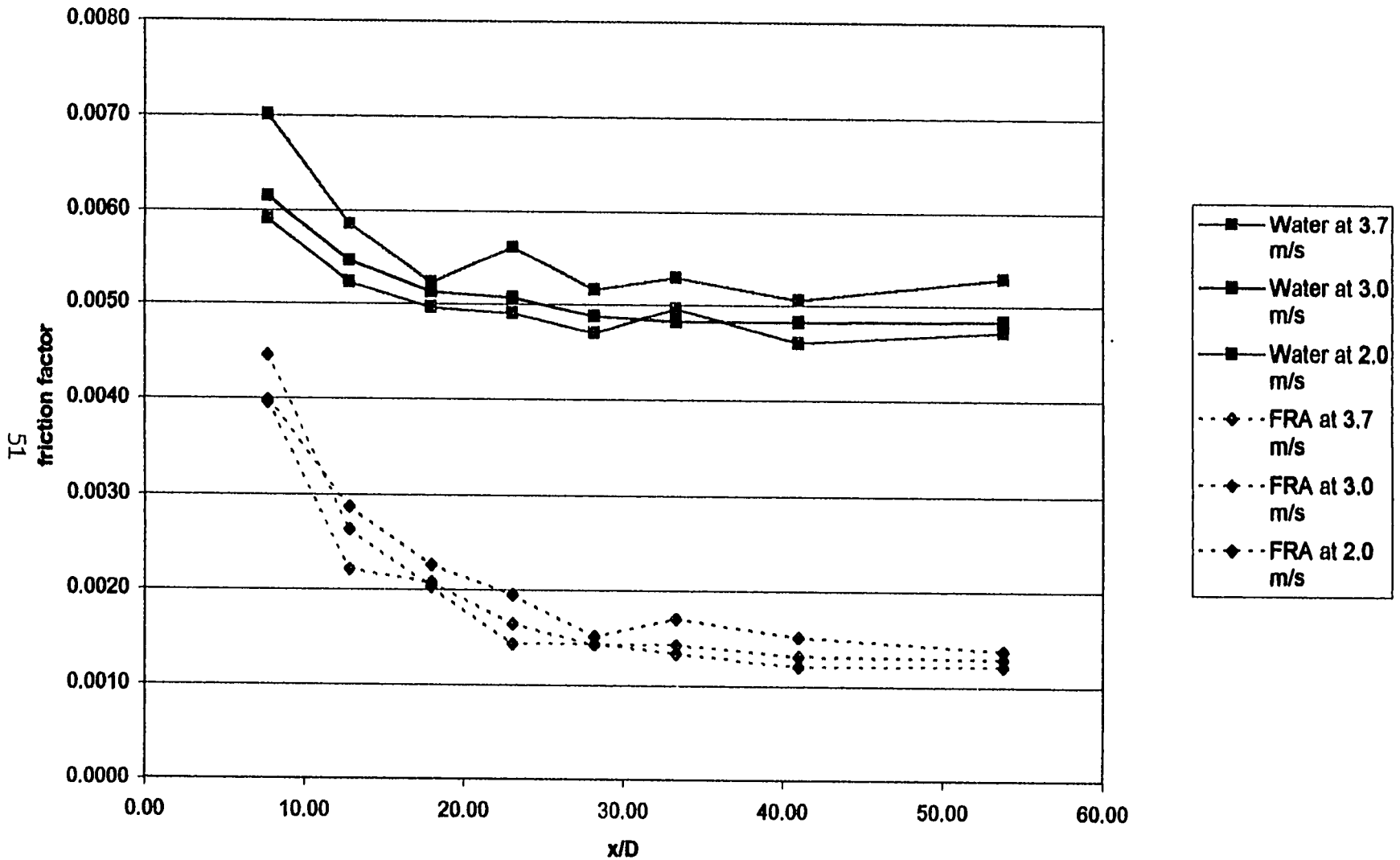

Figure 4.2 - Friction factor vs. x/D for FRA_2 with bigger hole obstruction at 50C

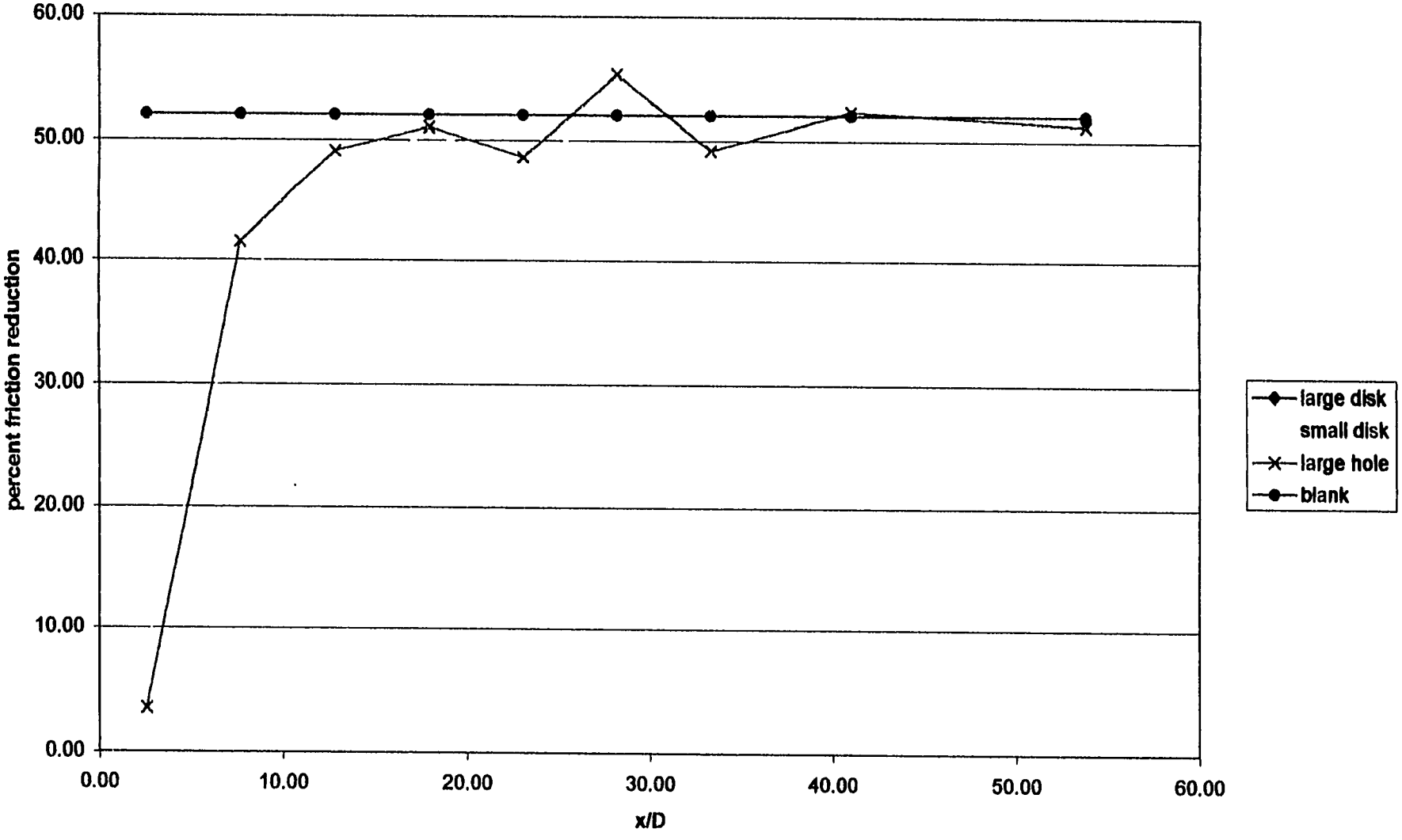

Figure 4.3 - Percent friction reduction vs. x/D for FRA1 for all obstructions at 40C - 3.7 m/s

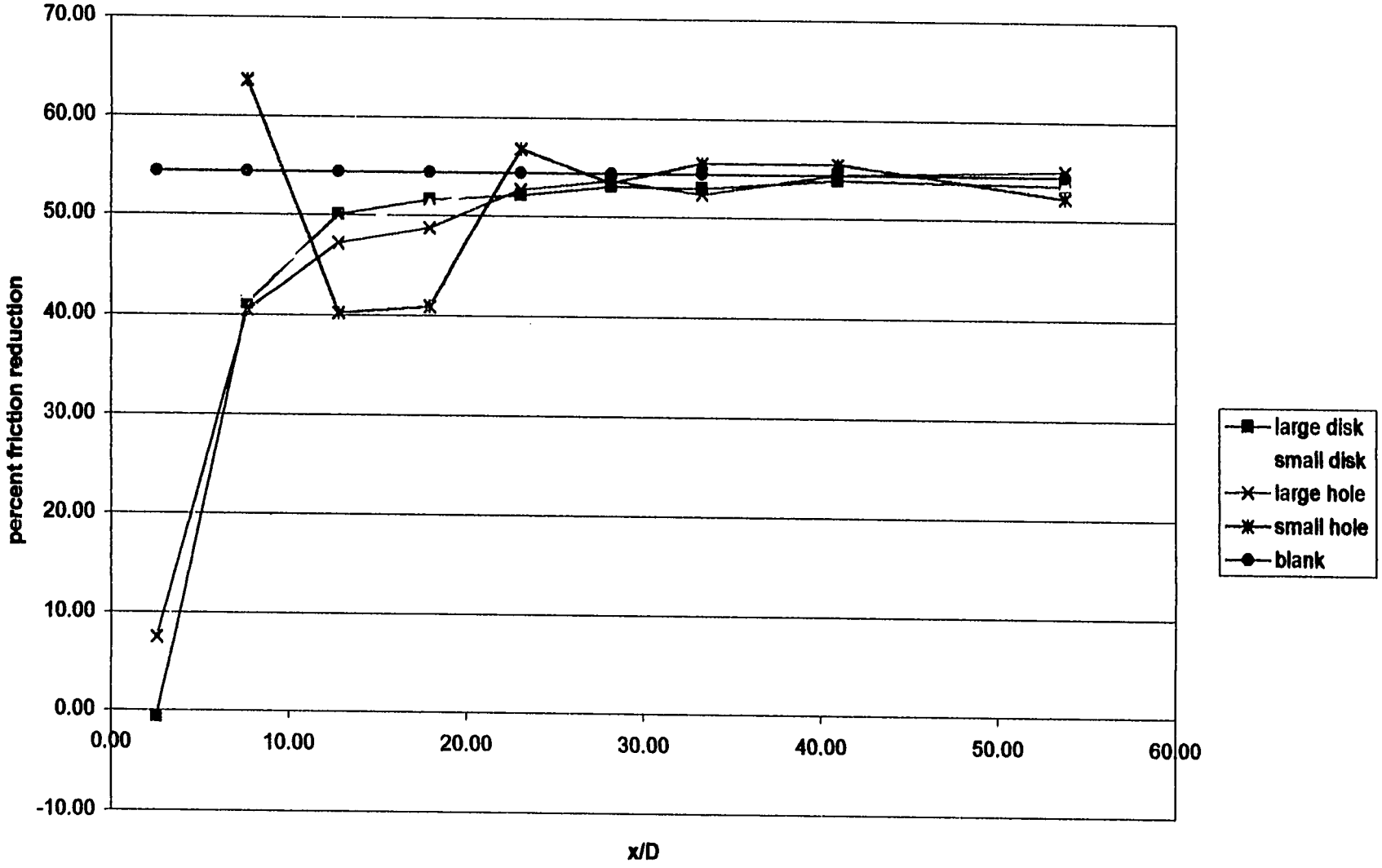

Figure 4.4 - Percent friction reduction vs. x/D for for FRA_1 for all obstruction plates at 40C - 3 m/s

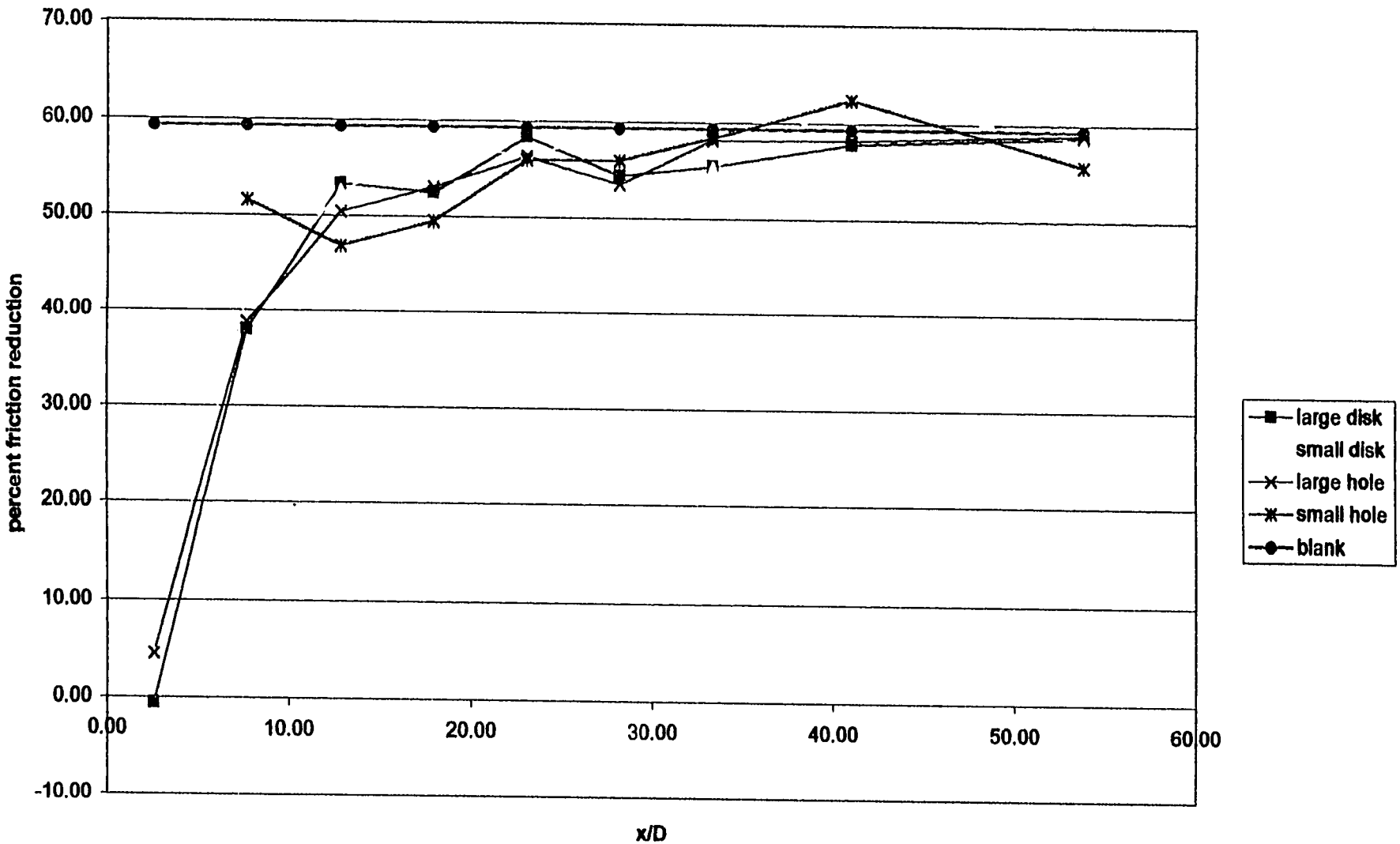

Figure 4.5 - Percent friction reduction vs. x/D for FRA1 for all obstruction plates at 40C - 2 m/s

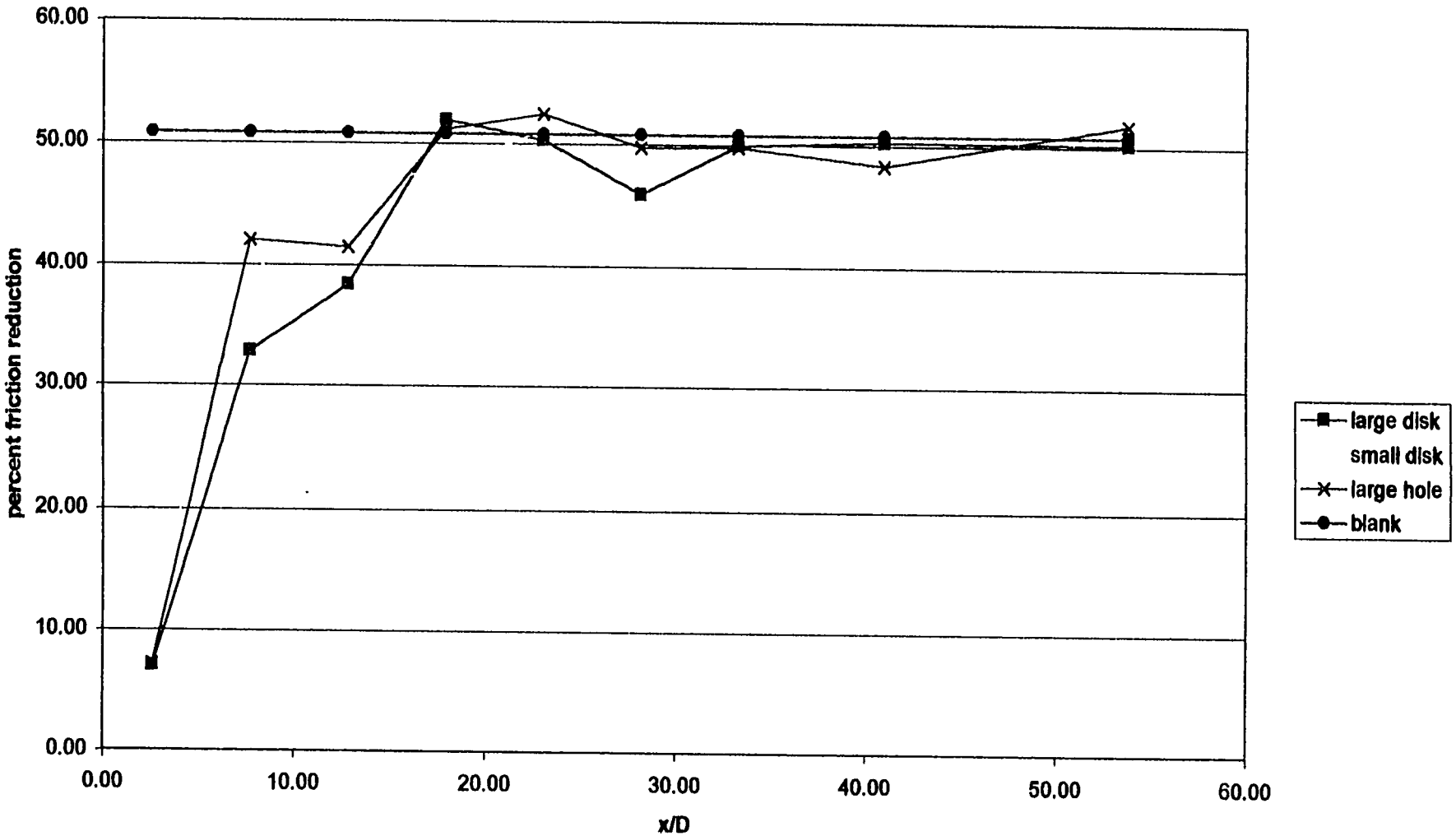

Figure 4.6 - Percent friction reduction vs. x/D for FRA1 for all obstructions at 50C - 3.7 m/s

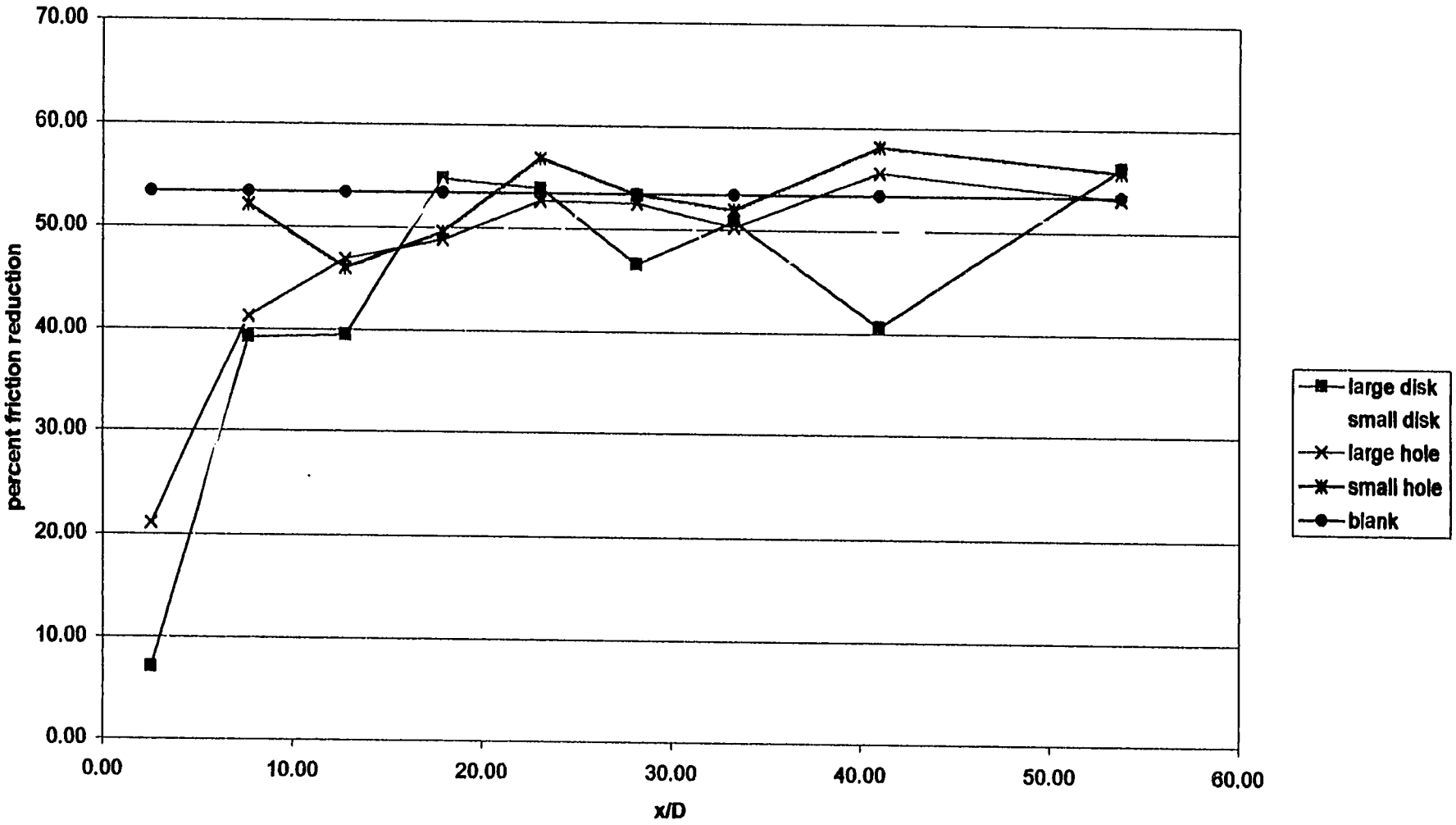

Figure 4.7 - Percent friction reduction vs. x/D for FRA1 for all obstruction plates at 50C - 3 m/s

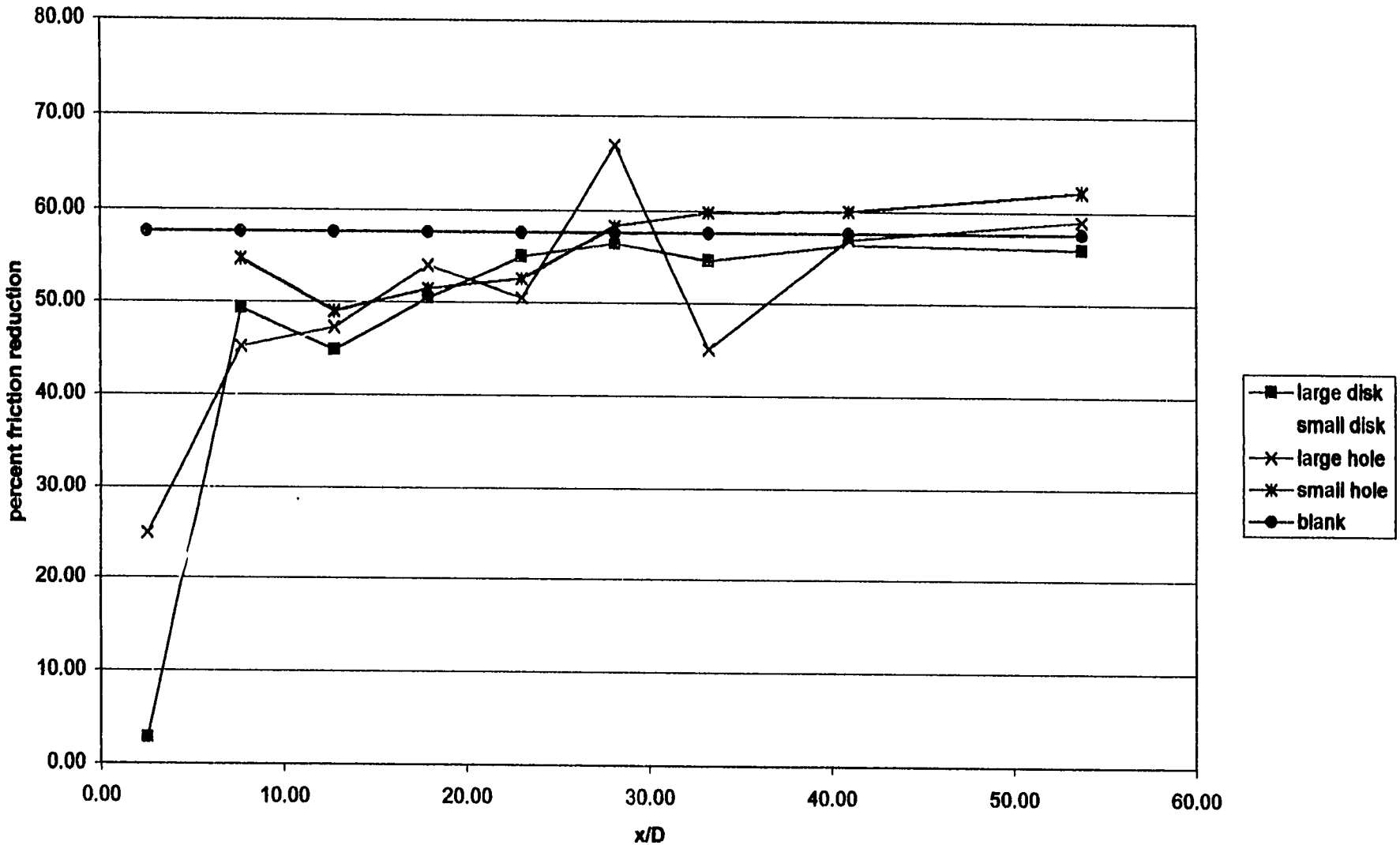

Figure 4.8 - Percent friction reduction vs. x/D for FRA_1 for all obstruction plates at 50C - 2 m/s

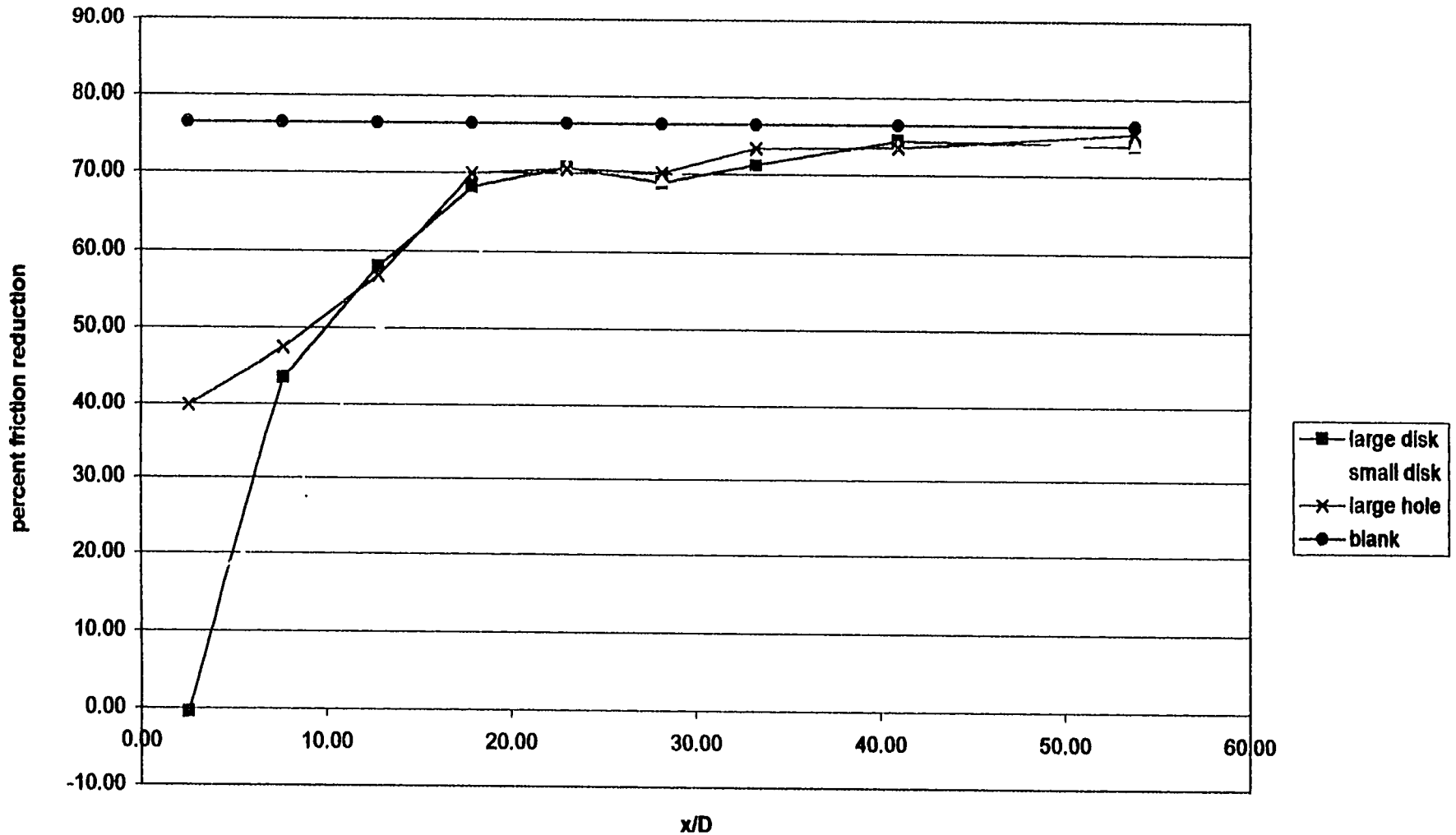

Figure 4.9 - Percent friction reduction vs. x/D for FRA2 for all obstructions at 50C - 3.7 m/s

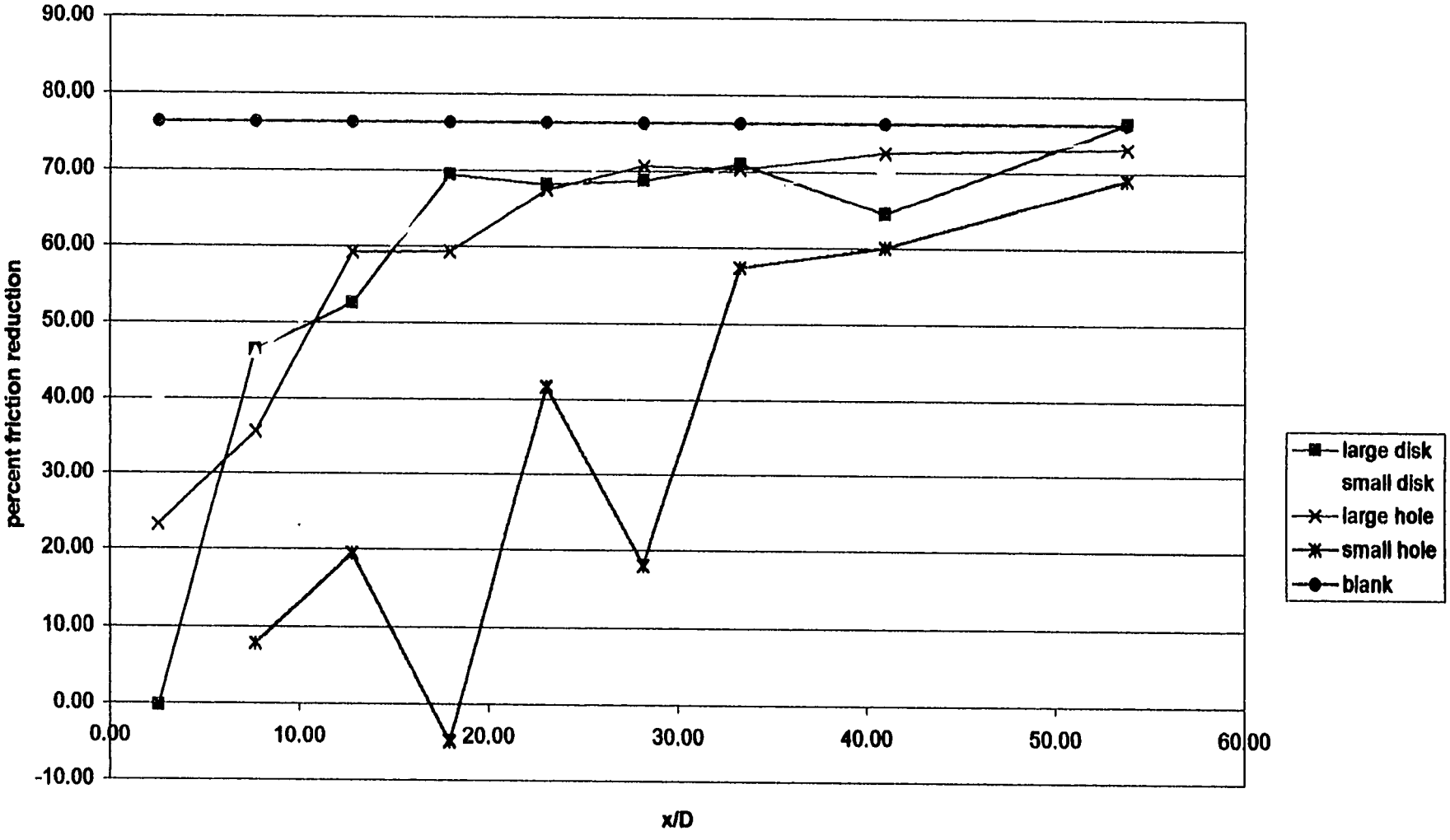

Figure 4.10 - Percent friction reduction vs. x/D for FRA2 for all obstruction plates at 50C - 3 m/s

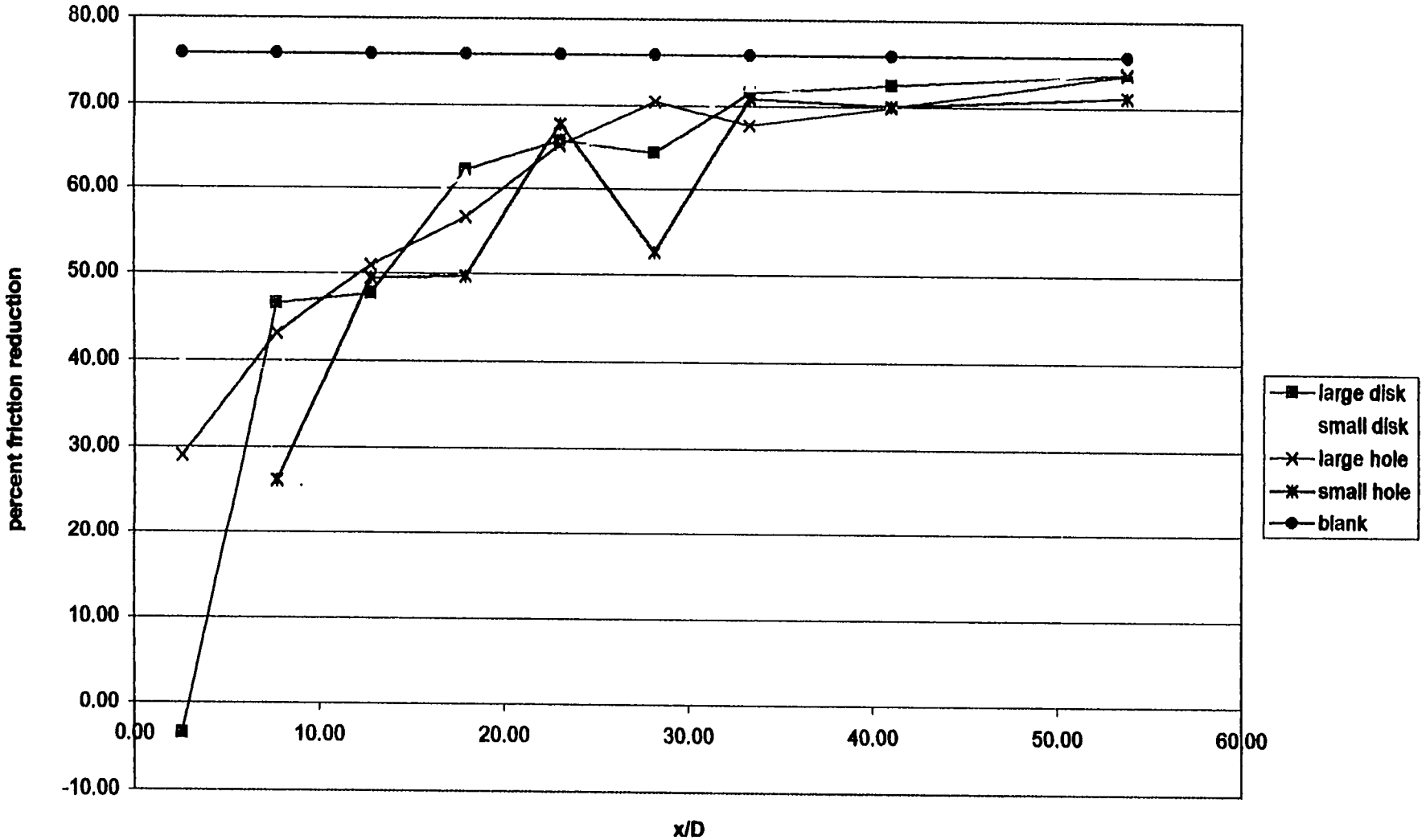

Figure 4.11 - Percent friction reduction vs. x/D for FRA2 for all obstruction plates at 50C - 2 m/s

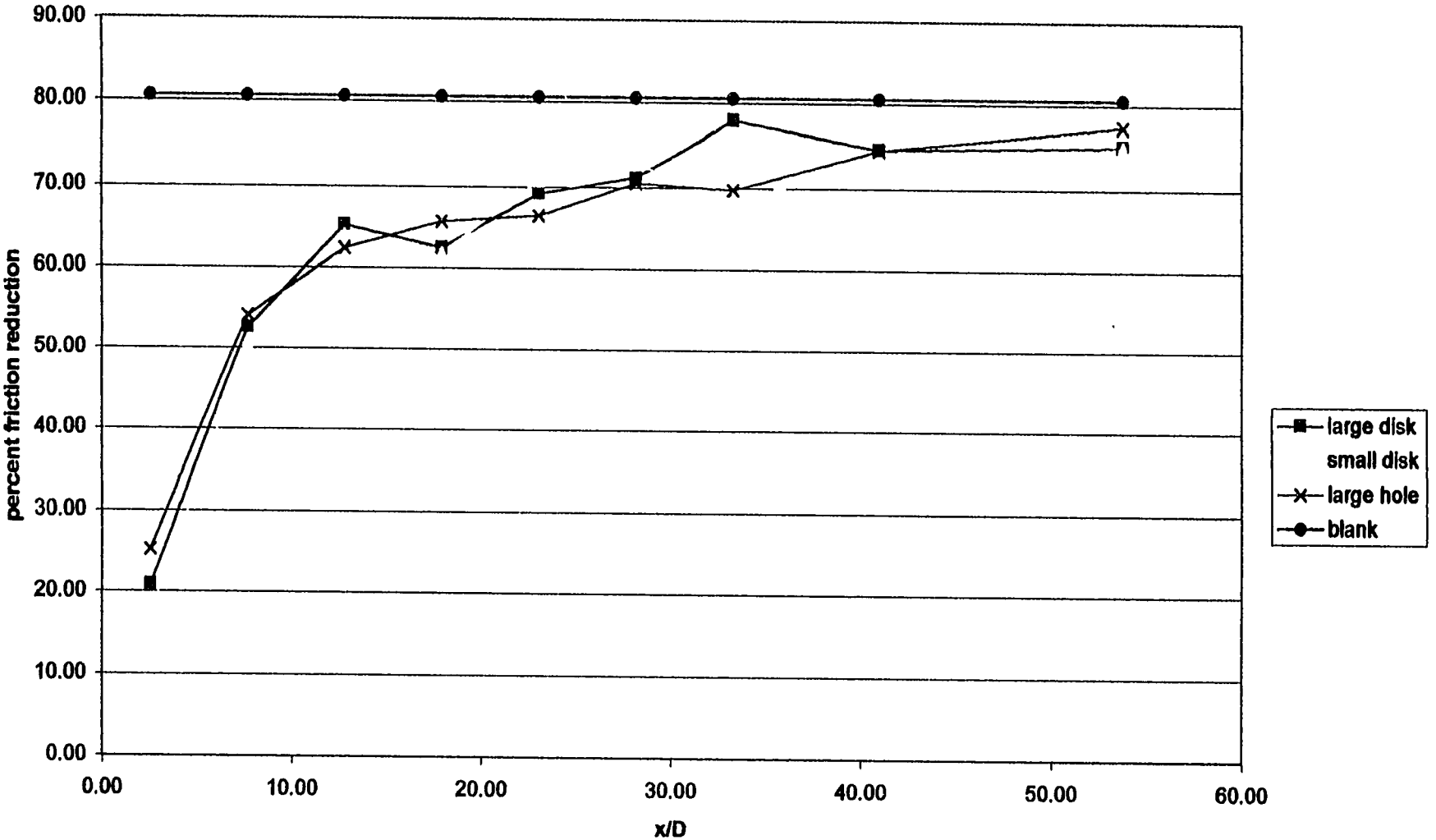

Figure 4.12 - Percent friction reduction vs. x/D for FRA2 for all obstructions at 70C - 3.7 m/s

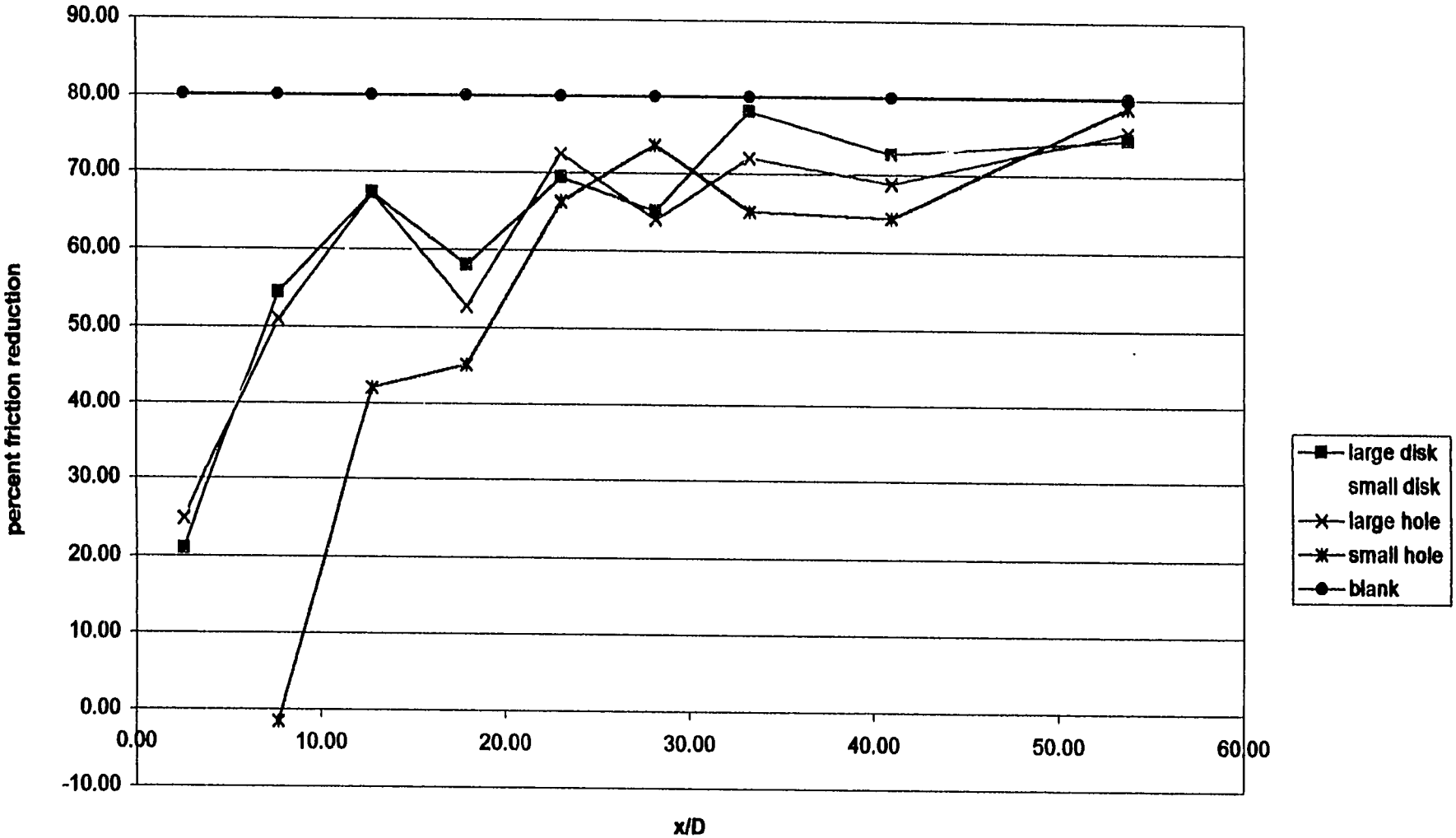

Figure 4.13 - Percent friction reduction vs. x/D for FRA2 for all obstruction plates at 70C - 3 m/s

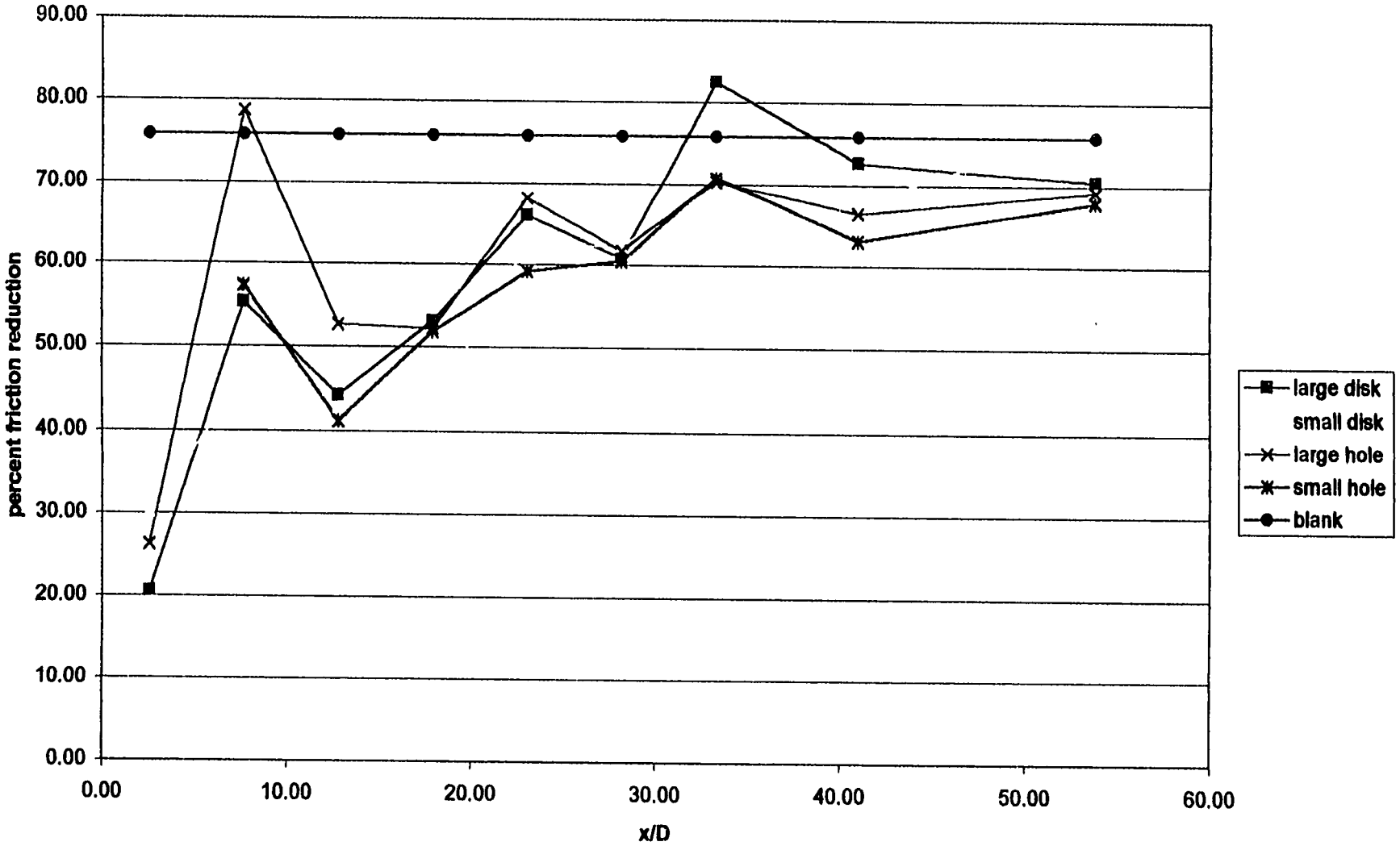

Figure 4.14 - Percent friction reduction vs. x/D for FRA2 for all obstruction plates at 70C - 2 m/s

Table 4.2 - Maximum friction reduction

Test run	Temperature and velocities	Percent friction reduction
1 - FRA_1	40°C - 3.7 m/s	52
	3.0 m/s	54
	2.0 m/s	59
2 - FRA_1	50°C - 3.7 m/s	51
	3.0 m/s	53
	2.0 m/s	58
3- FRA_2	50°C - 3.7 m/s	77
	3.0 m/s	76
	2.0 m/s	76
4-FRA_2	70°C - 3.7 m/s	81
	3.0 m/s	80
	2.0 m/s	76

laboratory tests with the additives. The only difference between the FRA_1 and FRA_2 samples was the alcohol solvent, which in the case of FRA_1 was isopropyl alcohol and in FRA_2 1,2-propanediol. It is possible that the presence of different third party 'spectator' species could affect the intermolecular attraction between surfactant molecules and interfere with the transformation from spherical to rod-like micelles which would in turn affect the extent of friction reduction. As well, the literature indicates that the order in which components are mixed may affect the effectiveness of the solution (Nash as

referenced in Shenoy, 1984). However, an identical mixing procedure was used for both preparations. To confirm the low friction factors measured for FRA_2 a second batch of the additive was prepared using the same components added in the same order. The resulting solution produced a maximum friction reduction of only 57%. Only one difference in experimental conditions remained: the first batch of FRA_2, which produced the 80% friction reduction, was added to the system at a temperature of 70°C, whereas the second batch was added at a temperature of 50°C and the water was then heated to 70°C. This experiment makes clear that it can be difficult to get completely reproducible results with different batches of the same FRA. No further results for the second batch of FRA_2 are shown here.

Also of note is that FRA_1 and the second preparation of FRA_2 (which produced only 57% drag reduction) completely and irreversibly lost their friction reducing effect after 48 hours, while the first preparation of FRA_2 was still completely effective after a week. Some authors (Gasljevic and Matthys, 1997, White and Zakin (as referenced in Shenoy, 1984)) have reported decreased effectiveness of surfactant-based friction reducing solutions with time. No explanations were offered for these observations of degradation.

In the present system, it was evident each time the tank was drained that a large amount of sediment was present. As well, there was clear evidence of rust, despite the selection of stainless steel components for the test loop. Some rusting on the internal surface of the storage tank was evident and it is possible that this could have interfered with the stability

of the micelles. It is also possible that there were contaminants, in particular suspended particulate matter, and calcium and magnesium ions, present in the tap water used to fill the system, which could have had similar effects.

Chemical analyses for atomic nitrogen through oxidative combustion and chemiluminescence detection were carried out on samples of the FRA solutions as an indication of the amount of surfactant present in the solution at the beginning and end of each test run. For every mole of surfactant, there should be one mole of nitrogen present. For a 4.2 mM solution of Ethoquad O/12, one would expect to measure a nitrogen concentration of 58 ppm, if all of the surfactant remains in the solution. With FRA_1, the nitrogen concentration was measured to be 24 ppm at the start of the test run and 20 ppm at the end of the run. FRA_2 samples had a nitrogen concentration of 47 ppm at the beginning and end of the test runs. This would seem to indicate that the increased effectiveness of FRA_2 could be due to a larger quantity of the surfactant remaining in the solution. The chemists performing these tests did express some concern about the accuracy of the results, however, because of the presence of sediment in the samples. The samples were shaken before microsamples were withdrawn for testing but there was no way to be sure of uniformity within the microsamples.

Despite the inconsistency in maximum friction reduction between FRA_1 and FRA_2, the samples themselves did result in consistent and reproducible value of maximum friction reduction. The values of maximum friction reduction for each set of data in Table 4.1 are

within the range of experimental error for friction reduction.

4.2.2 Recovery of Friction Reduction

Figures 4.3 to 4.14 show large scatter in the data for percent friction reduction, particularly for the lowest velocity (2 m/s). The higher degree of scatter at lower velocities is due to the greater impact of the errors in pressure difference on friction factors, as well as the larger relative contribution of errors in the flow rate, as can be seen from the error calculations in Appendix B.

In comparing obstruction plates for a given velocity, significant scatter is observed for the small hole obstruction plate data and also on occasion for the large hole. This may be due to the presence of an unsymmetrical re-attachment of the central jet downstream of the orifice, or of unsteady flow with large periodic vortices. One of the most striking observations is that the geometry of the obstruction appears to have little effect on the recovery distance (i.e. the distance for the percent friction reduction to reach the asymptotic value) and that this distance is consistent for all velocities and in the range of 25-30 diameters. These values are very similar to those obtained by Gasljevic and Matthys (1997) in their work with porous plug and conical entry obstructions at the low flow rates they examined (1.5 and 2.1 m/s). However, they obtained much higher recovery distances of 100 diameters and greater at the highest flow rates examined, presumably because at these shear stresses breakdown of the SIS was taking place. This effect was observed

with the obstruction creating the greatest shear in this experiment, the small hole, with FRA_2 at the higher of the two velocities examined with this obstruction (Figures 4.10 and 4.14). It is likely that the same effect is occurring here also: the greater shear is creating breakdown of the micelles in addition to the SIS and this is delaying recovery. The other obstructions do not create sufficient shear to cause this to happen. This breakdown of the SIS was accomplished with a pressure losses in the order of 2000-3000 diameters, comparable to values reported by Gasljevic and Matthys (1997).

4.3 Model for FRA Recovery

It is remarkable that in most of the data presented here, neither the flow velocity nor the obstruction geometry seems to affect the length required for recovery. Only the highest velocity with the small hole brought any deviation from this. This section develops a simple model which explains this finding.

As indicated in the discussion above, friction reduction effectiveness can be defined by

$$\eta = \frac{f_{solvent} - f_{fra}}{f_{solvent}} \cdot 100\% \qquad (4.2)$$

Figures 4.3 to 4.14 show that after a developing length, η approaches a maximum value, η_∞. If η is proportional to the concentration of micelles combined in the shear induced state (SIS) in the solution and $(\eta_\infty - \eta)$ is proportional to the concentration of micelles not yet combined in friction reducing structures, and the "reaction" of micelles to form the SIS

is considered to be first order in the amount of "unreacted" micelles, then the rate of formation of the SIS or the rate of initiation of friction reduction can be represented as:

$$\frac{d\eta}{dt} = k(\eta_\infty - \eta) \qquad (4.3)$$

Solving this equation,

$$\frac{\eta_\infty - \eta}{\eta_\infty - \eta_0} = \exp(-kt) \qquad (4.4)$$

but $\eta_0 = 0$, therefore,

$$\eta = \eta_\infty(1 - \exp(-kt)) \qquad (4.5)$$

Hu and Matthys (1985) presented data from rheometer measurements on the time required to produce a shear-induced state (SIS) as a function of shear rate. They identified two characteristic times: an induction time t_I, during which no effects of shear on the viscosity or first normal stress difference are seen; and a "plateau" time t_S, during which the viscosity climbs rapidly and approaches an asymptote as the SIS is formed. The behaviour during the "plateau" time closely resembles equation 4.5. When the SIS is broken down by shear, reformation takes place after a time t_s. No induction time t_I is required to re-form the SIS after breakdown unless the fluid experiences very high shear stresses. Only with very high shear, such as was produced by Gasljevic and Matthys (1997) with a wire mesh plug, is an induction time apparently needed to reform the SIS. It is speculated that during the induction time, small primary aggregates of micelles are formed, which are subsequently assembled into the SIS. A shear sufficient to break down the SIS does not

normally affect the primary aggregates; these can, however, be broken down by very high

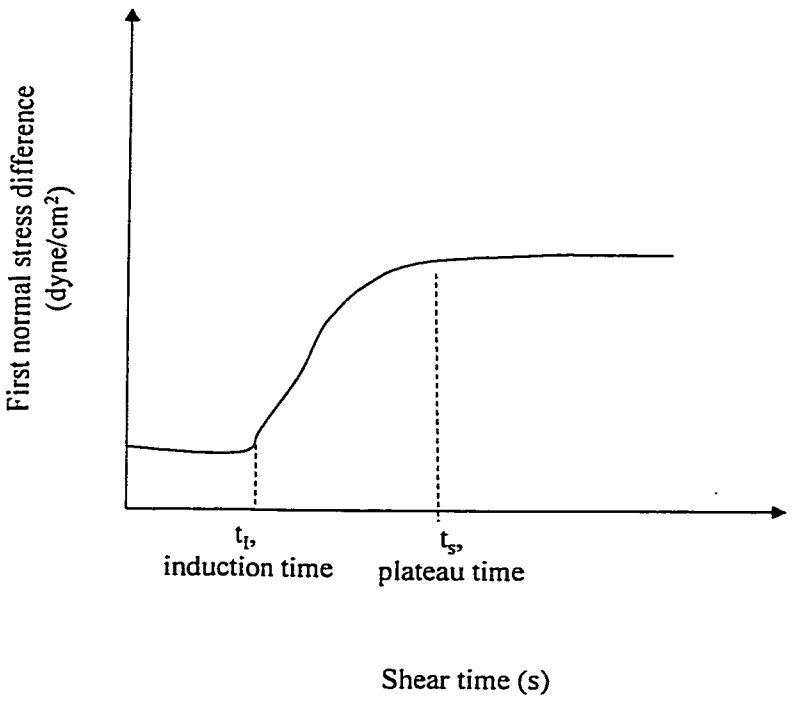

Figure 4.15 - First normal stress difference vs. shear time
(After Hu and Matthys, 1995)

shear, in which case an induction time is necessary to re-form them before the SIS can be reassembled.

In this experiment, with the exception of flow through the small hole obstruction plate at the highest velocities examined (3.0 m/s), the plateau time appeared to be equal to the recovery time. That is, the shear stresses were not high enough to cause breakdown of the primary micelle aggregates in nearly all of the experimental runs presented here.

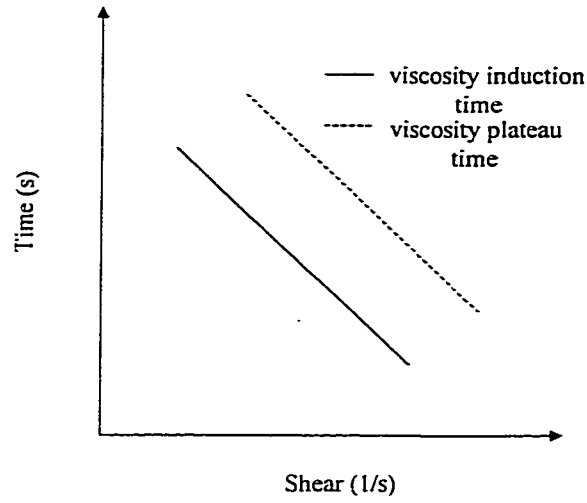

Figure 4.16 - Induction and plateau times for shear viscosity vs. shear rate (After Hu and Matthys, 1995)

Hu and Matthys (1995) found that the log of the plateau time, t_s, and induction time, t_i, varied inversely with the log of the shear rate of the fluid.

The relationship that they described can also be expressed in the form :

$$\ln t_s = \ln A + B \ln \gamma \quad (4.6) \quad \text{or}$$

$$t_s = A\gamma^B \quad (4.7)$$

For a characteristic velocity in the flow downstream of the obstruction described by V and a characteristic shear layer thickness δ, the shear rate in the recovery region can be expressed as:

$$\gamma = \frac{V}{\delta} \quad (4.8)$$

If one defines a recovery time as the time for η, the percent friction reduction or FRA effectiveness, to reach 95% of η_∞, the maximum friction reduction (also equal to t_s), then, following from equation 4.5,

$$k\, t_s = 3 \quad (4.9)$$

In other words, recovery is deemed to have taken place in 3 time constants. Combining from equations 4.7 to 4.9,

$$k = \frac{3\delta^B}{AV^B} \quad (4.10)$$

Equation 4.3 above can be rewritten, substituting V δt for δx:

$$\frac{d\eta}{d(x/D)} = \frac{D}{V}\frac{d\eta}{dt} = K(\eta_\infty - \eta) \quad (4.11)$$

where K is equal to kD/V. The solution of equation 4.11 is:

$$\eta = \eta_\infty (1 - \exp(-K\frac{x}{D})) \quad (4.12)$$

Friction reduction effectiveness profile data for all experimental runs were fitted to this equation and the following values shown in Table 4.3 were obtained for K. Sample plots of the experimental data and fitted curves appear in Figures 4.17 and 4.18.

Table 4.3 - K values for friction reduction effectiveness recovery curve fitting

	Bigger disk	Smaller disk	Bigger hole	Smaller hole
FRA1 at 40°C				
3.7 m/s	-0.070	-0.067	-0.062	
3.0 m/s	-0.068	-0.067	-0.061	-0.064
2.0 m/s	-0.064	-0.064	-0.059	-0.054
FRA1 at 50°C				
3.7 m/s	-0.080	-0.089	-0.075	
3.0 m/s	-0.074	-0.089	-0.073	-0.035
2.0 m/s	-0.075	-0.078	-0.071	-0.062
FRA2 at 50°C				
3.7 m/s	-0.083	-0.10	-0.10	
3.0 m/s	-0.074	-0.057	-0.079	-0.081
2.0 m/s	-0.093	-0.13	-0.047	-0.094
FRA2 at 70°C				
3.7 m/s		-0.069	-0.10	
3.0 m/s	-0.11	-0.096	-0.12	-0.051
2.0 m/s	-0.096	-0.072	-0.10	-0.066

To relate these fits to Hu and Matthys' (1995) values of t_s, let us return to equation 4.10. V is taken to be a characteristic velocity for the shear layer downstream of the obstruction, and is a constant equal to the average of the velocity V_s (velocity at the obstruction) and V_0 (velocity in the unobstructed pipe).

$$V = \tfrac{1}{2} (V_s + V_0) \qquad (4.13)$$

The picture behind this model is that of a jet or wake flow emerging from the obstruction at V_s and linearly expanding to V_0. These two velocities can be related by the ratio of blockage in the tube (which would be, for example, 0.5 for the large hole obstruction and 0.75 for the small hole obstruction).

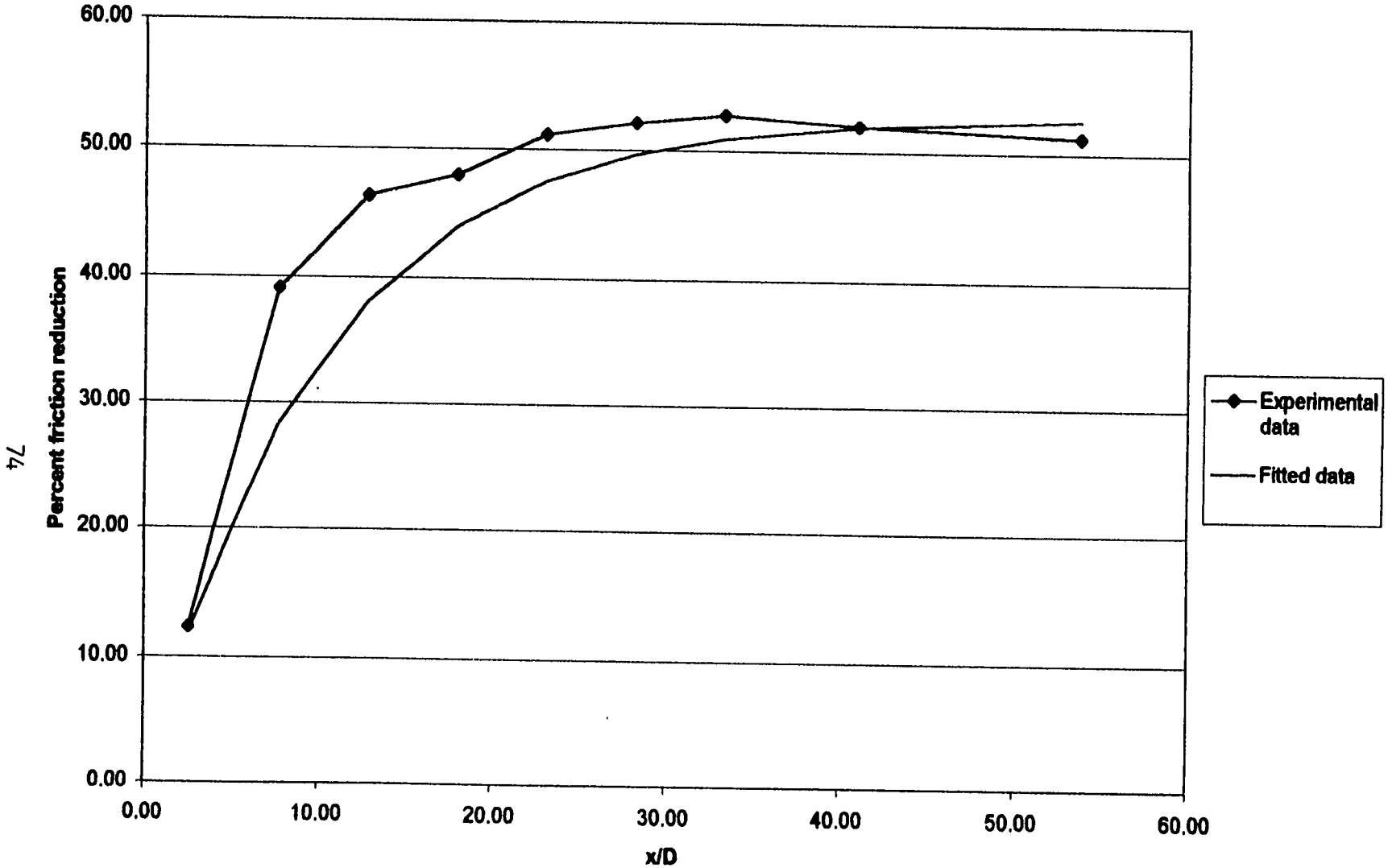

Figure 4.17 - Percent friction reduction vs. x/D for FRA_1 with bigger hole obstruction
at 50°C and 3.7 m/s

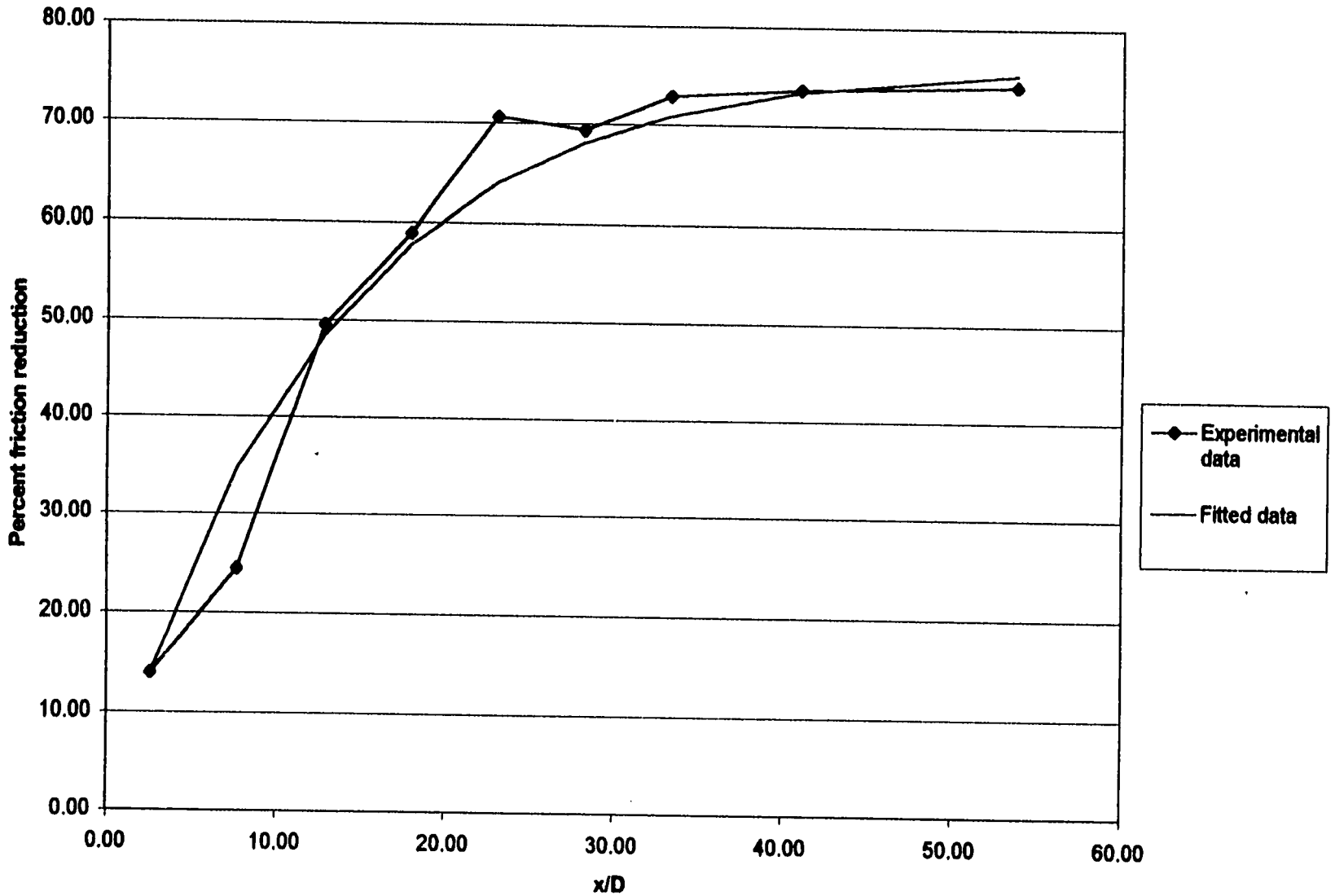

Figure 4.18 - Percent friction reduction vs. x/D for FRA_2 with bigger hole obstruction
at 50°C and 3.7 m/s

$$b=A_{obstruction}/A_{pipe} \quad (4.14)$$

Then V_s can be described as V_0/b, or

$$V = V_o\left(\frac{1+b}{2b}\right) \quad (4.15)$$

A final expression can then be derived for K:

$$K = \frac{3\delta^B D}{A\left(V_0(1+b)/2b\right)^{B+1}} \quad (4.16)$$

When equation 4.7 is fitted to the two sets of data presented by Hu and Matthys (1995) for time vs. shear rate, the following coefficients are obtained (Table 4.4) for a similar, but not identical, FRA to the ones used here. The values of B are close to -1, indicating a weak dependence of K on velocity and blockage.

Table 4.4 - Coefficients for equation 4.7
derived from Hu and Matthys' (1995) data

	First normal stress difference	Shear viscosity
A	10250	7510
B	-0.83	-0.72

A value for B of -1 gives the re-formation time as being directly proportional to the inverse of the velocity, so that the distance required for the SIS to recover would be constant as velocity increases. With this value of B, equation 4.16 above becomes,

$$K = 3D/A\delta \quad (4.17)$$

The weak or zero dependence of the rate parameter K given by equation 4.16 on 4.17 on velocity and blockage ratio explains why no significant effect of these factors on friction reduction has been found in these experiments. In physical terms, a higher shear rate, produced either by a greater blockage or a higher flow rate, also leads to faster re-formation of the SIS and recovery of drag reduction. The effects of velocity on recovery and distance travelled therefore cancel out. The exact value of the exponent B for the present surfactant is not known, but it appears to be close to -1. Gasljevic and Matthys (1997) also found that velocity did not affect recovery lengths.

As a further test of this theory, fitted values of K can be substituted into equation 4.16 and the coefficients from Table 4.4 used to solve for the shear layer thickness δ. This produces a shear layer thickness of $\delta \approx 0.85$ mm for the large hole and large disk obstructions (where b=0.5) and $\delta \approx 1.0$ mm for the small hole obstruction (where b=0.25), based on Matthys' first data set and with $V_0 = 3$ m/s. These appear to be reasonable numbers for the thickness of the shear region at the edge of the jet emerging from the obstruction.

In Figures 4.10 and 4.13 (the small hole obstruction with FRA_2 for the 50°C and 70°C experimental runs) the behaviour at 3.0 m/s is obviously different and appears to take the form of Figure 4.15 with a non-zero induction time. These are similar to the high

shear/wire mesh plug results of Gasljevic and Matthys (1997) although their recovery distances are much greater. These curves can be roughly fitted by an equation of the form,

$$\eta = \eta_{\infty}\left(1-\exp\left(-K\left(\frac{x}{D}-\frac{x_0}{D}\right)\right)\right) \quad (4.18)$$

(Figures 4.19 and 4.20) where x_0 is a delay distance, which should be related to t_l by x_0=V x t_l. Although the scatter is very large, equation 4.18 seems to be a reasonable representation.

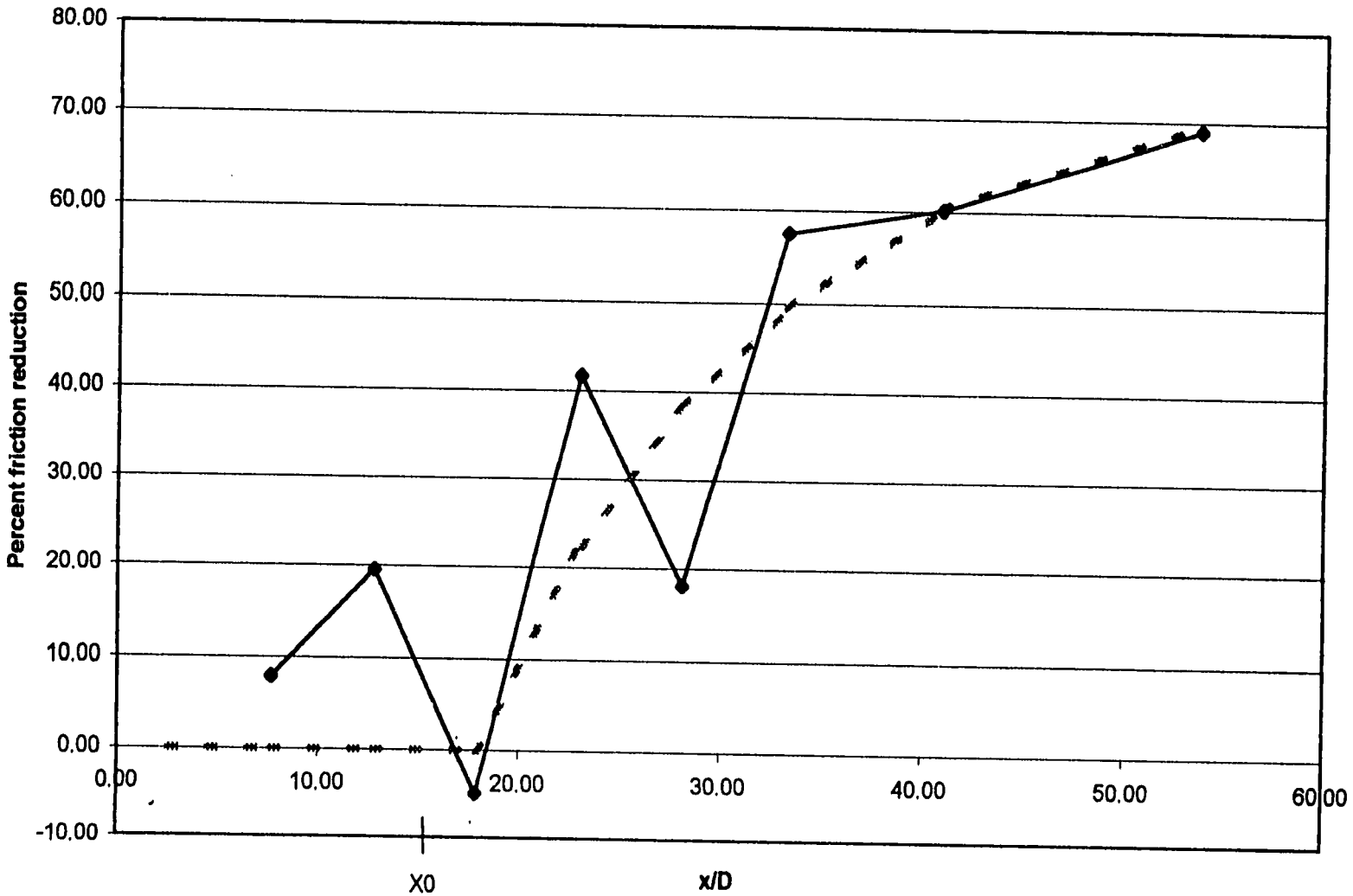

Figure 4.19 - Percent friction reduction vs. x/D for FRA_2 with smaller hole obstruction at 50C and 3 m/s

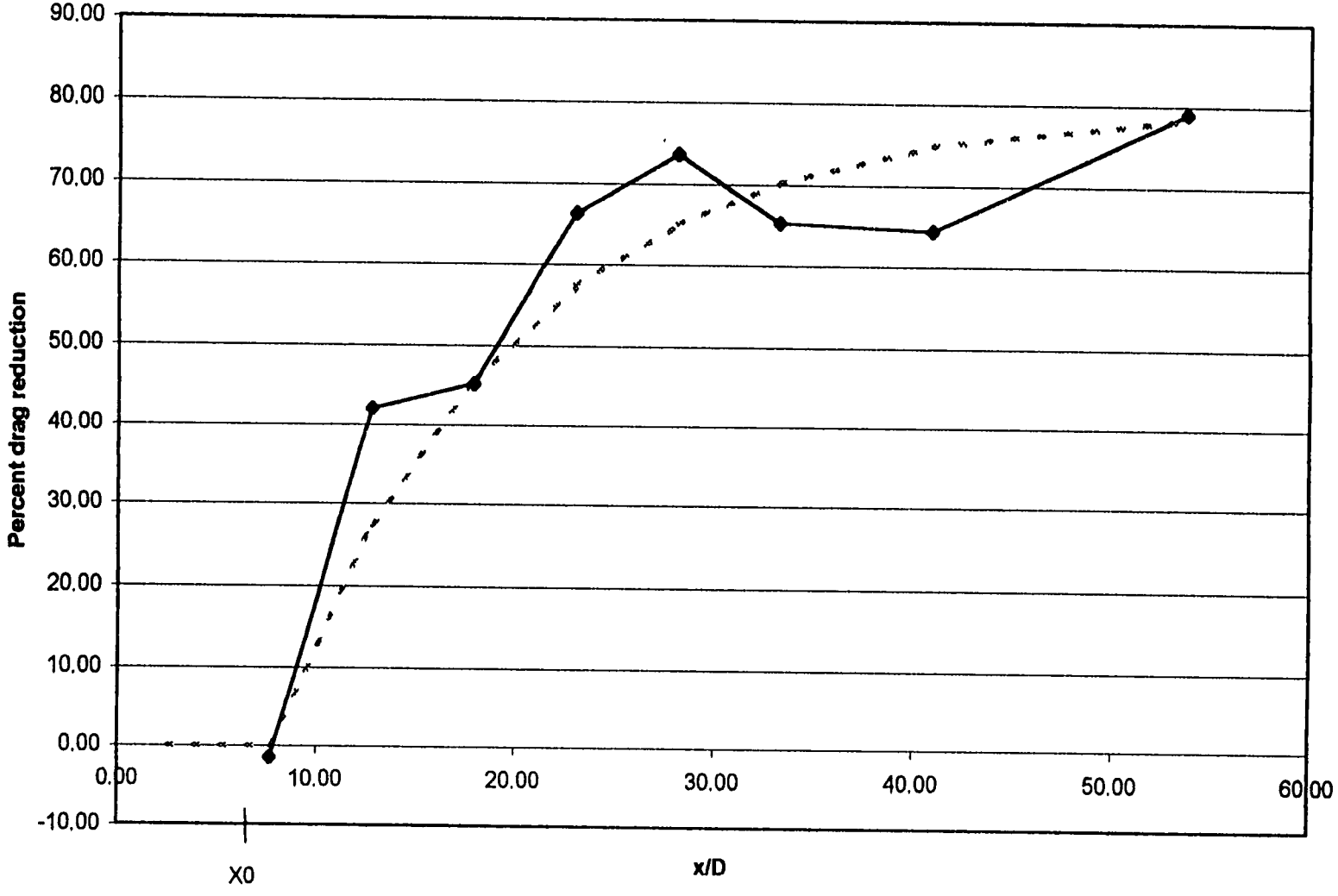

Figure 4.20 - Percent friction reduction vs. x/D for FRA_2 with smaller hole obstruction at 50C and 3 m/s

5.0 Conclusions and Recommendations

The goal of this research project was to evaluate whether micelles formed in surfactant friction reducing solutions can be broken down with moderate pressure losses in order to restore friction losses in pipe to normal levels and recover heat transfer. To do this, a series of four obstructing devices were designed and tested for their ability to reverse the friction reducing effect. Pressures were measured across and downstream of the four obstruction plates for the FRA solution and for water in order to draw conclusions about recovery distances and the relative effectiveness of the obstruction geometries. A quaternary ammonium surfactant, Ethoquad 0/12-H (FRA_1) and Ethoquad 0/12-PG (FRA_2) were used in this experiment with 3-hydroxy-2-naphthoate as the counterion, with a surfactant concentration of 1600 ppm and a counterion concentration of 800 ppm.

For pressure drop measurements of water with the blank obstruction (open tube experiments) excellent agreement was measured with published friction factors. This gives a high degree of confidence in the experimental method and in the data reduction procedure.

Average friction reduction of 55% was measured with FRA_1, consistent with values reported by Young (1995). With one of the batches of FRA_2, the measured average friction reduction dramatically exceeded these values (78%). Recovery distances of 25-30 diameters were measured for all test conditions except for two. Recovery was delayed

beyond 30 diameters for FRA_2 with the small hole obstruction at the highest velocity measured, 3.0 m/s.

The differences in maximum friction reduction with FRA_1 and FRA_2 could be attributable to differences in the water chemistry for that particular run, differences in third party spectator species, or differences in mixing procedures. Tests measuring the nitrogen concentration indicated a higher amount of nitrogen in the first batch of FRA_2. This may reflect a greater concentration of surfactant present in the solution. Further work into the chemistry behind the observed effects is recommended. It is also recommended that preliminary tests to screen samples are carried out on a very small scale before additives are tested in the 360L test loop. It would also be worthwhile carrying out rheometer measurements on the FRAs tested in order to establish values for B in equation 4.16, which is an indication of the relationship between the re-formation time and the velocity. From the data evaluated, B appears to lie close to -1, indicating recovery distances which are independent of the velocity. Matthys and Sabersky (1982) noted the difficulty in scaling friction reduction measured in tubing of a given diameter to a different diameter. It would be worth investigating this effect in pipes of different diameters before the friction reducing additive is added to actual systems, to ensure that the predicted friction reduction and benefits will take place.

The model presented in section 4.3 has been developed with data presented by Hu and Matthys (1995) and is consistent with the observations in this experiment that the recovery

distance is independent of the velocity and independent of the obstruction geometry. The model allows estimation of the shear layer thickness downstream of the obstruction. These values were 0.85 mm for the large hole and large disk obstructions and 1.0 mm for the small hole obstruction.

Only one set of experimental conditions produced sufficient shear to result in breakdown of the micellar shear-induced state (the secondary structures). The breakdown resulted for flow of FRA_2 through the small hole obstruction plate at the highest velocities tested (3 m/s). In all other test runs, the recovery distances measured are consistent with results in the literature and are in the order of 30 diameters (Gasljevic and Matthys, 1997). It is recommended that further examination of micellar disruption be carried out at higher velocities. In this test loop, that will require a more powerful pump and a flow meter and pressure transducers with a greater operating ranges. Of greater importance still, is the repetition of parts of this experiment while measuring temperatures along the test section in order to confirm that the breakdown of micelles does indeed produce measurable increases in heat transfer coefficients.

6.0 References

1. Althaus, Wilhelm, and Schiffmann, Jürgen, "Increasing the Capacity of DH Transport Lines with Smooth Water", *Fernwärme International*, **24**: 193-220 (1995).

2. Althaus, W., Steiff, A., and Wefels, P., "Drag Reducing Additives in District Heating - Chance or Fantasy", *Proceedings of the 7th Int'l Symp. on DHC*, May 18-20, 1-24 (1999).

3. Baron, A., Quadrio, M., and Vigevano, L., "On the Boundary Layer/Riblets Interaction Mechanisms and the Prediction of Turbulent Drag Reduction", *Int. J. Heat and Fluid Flow*, **14**: 324-332 (1993).

4. Bewersdorff, H.W., and Thiel, H., "Turbulence Structure of Dilute Polymer and Surfactant Solutions in Artificially Roughened Pipes", *Applied Scientific Research*, **50:** 347-368 (1993).

5. Bewersdorff, H.W., Dohmann, J., Langowski, J., Lindler, P., Maack, A., Oberthuer, R. and Thiel, H., "SANS- and LS-studies on Drag-Reducing Surfactant Solutions", *Physica B*, **156 & 157:** 508-511 (1989).

6. Bewersdorff, H.W., and Ohlendorf, D., "The Behaviour of Drag-Reducing Cationic Surfactant Solutions", *Colloid Polym Sci.*, **266**: 941-953 (1988).

7. Bird, R., Stewart, W. and Lightfoot, E., Transport Phenomena (1960).

8. Blais, C., Harwigsson, I., Hellsten, M., Wollerstrand, J., "Drag Reduction in District Heating and Cooling Circuits - Temporary Disruption of Micelles to Preserve the Heat Exchanger Capacity", *International District Energy Conference Proceedings*, **87:** 239-253 (1996).

9. Chara, Z., Zakin, J., Severa, M. and Myska, J., "Turbulence Measurements of Drag Reducing Surfactant Systems", *Experiments in Fluids*, **16**: 36-41 (1993).

10. Cho, Y.I. and Hartnett, J.P., "Non-Newtonian Fluids in Circular Pipe Flow", *Advances in Heat Transfer*, **15:** 59-134 (1982).

11. Choi, E., Cho, Y.I., "Local Friction and Heat Transfer Behaviour of Water in a Turbulent Pipe Flow with a Large Heat Flux at the Wall", *Journal of Heat Transfer*, **117:** 283-288 (1995).

12. Chou, L.C., Christensen, R.N., and Zakin, J.L., "The Use of Cationic Surfactant Additives to Reduce Transmission Pumping Costs in District Heating Systems", *Proc. Int. Dist Heating & Cooling Assoc*, **78**: 284-294 (1987).

13. De Groot, M.C. and Kievit, E.A., "The Effect of Surfactants on Domestic Heat Exchangers for Hot Water Supply and Heat Flow Meters in D/H Systems", *Advanced Energy Transmission Fluids for District Heating and Cooling, International Energy Agency Programme of Research, Development and Demonstration on District Heating and Cooling*, **N2:** B1-B94 (1996).

14. Dodge D.W., and Metzner, A.B., "Turbulent Flow of Non-Newtonian Systems", *A.I.Ch.E. Journal*, **5**: 189-204 (1959).

15. Earth Spring Resources, Ltd., "Advanced Fluids for District Heating and Cooling Energy Transmission: A Summary of Research and Testing Activities Carried out by International Energy Agency Member Researchers", *Advanced Energy Transmission Fluids, International Energy Agency Programme of Research, Development and Demonstration on District Heating*, **R-9**: 7-1 - 7-24 (1990).

16. Fabula, A.G., Hoyt, J.W., and Crawford, H.R., "Turbulent Flow Characteristics of Dilute Aqueous Solutions of High Polymers", *Bulletin, American Physical Society*, **8**: 25-27 (1963).

17. Fankhänel, M., Althaus, W., Steiff, W and Weinspach, P., "On the Influence of Drag Reducing Additives on Pressure Drop and Heat Transfer in District Heating Systems" *Proc. Int. Dist Heating & Cooling Assoc*, **78**: (1987).

18. Fankhänel, M., Icking, M., Althaus, W., Steiff, A., Weinspach, P., "Hydraulic Network Simulation of the Use of Drag Reducing Additives in District Heating Systems", *International Symposium on District Heat Simulation, Reykjavik, Iceland*, April 13-16, 1989.

19. Forrest, G., *Paper Trade Journal*, **22**: 298-303 (1931).

20. Fossa, M., Tagliafico, L.A., "Experimental Heat Transfer of Drag Reducing Polymer Solutions in Enhanced Surface Heat Exchangers", *Experimental Thermal and Fluid Science*, **10**: 221-228 (1995).

21. Gasljevic, K., and Matthys, E.F., "A Feasibility Study of the Use of Drag Reducing Additives to Reduce Pumping Power in Hydronic Thermal Distribution Systems", *Industrial Applications of Fluid Mechanics*, ASME, **FED 132**: 57-65 (1991).

22. Gasljevic, K., and Matthys, E.F., "Hydrodynamic and Thermal Field Development in the Pipe Entry Region for Turbulent Flow of Drag-reducing Surfactant Solutions", *Proceedings of the 1994 International Mechanical Engineering Congress and Exposition*, **206:** 51-61 (1994).

23. Gasljevic, K., Nan, X, and Matthys, E.F., "Effect of Drag-Reducing Surfactant Additives on Heat Exchangers", *Proceedings of the 1993 ASME Winter Annual Meeting*, **175:** 101-108 (1993).

24. Gasljevic, K., and Matthys, E.F., "Effect of Drag-Reducing Surfactant Solutions on Centrifugal Pumps Performance, Winter Annual Meeting of the American Society of Mechanical Engineers, **153**: 49-56 (1992).

25. Gasljevic, K., and Matthys, E.F., "On Saving Pumping Power in Hydronic Thermal Distribution Systems Through the Use of Drag-Reducing Additives", *Energy and Buildings*, **20:** 45-56 (1993).

26. Gasljevic, K., and Matthys, E.F., "Experimental Investigation of Thermal and Hydrodynamic Development Regions for Drag-Reducing Surfactant Solutions, *Journal of Heat Transfer*, **119**: 80-88 (1997).

27. Ghajar, A., and Yoon, H., "A Heat Transfer Correlation for Viscoelastic Turbulent Pipe Flows", *Chem Eng. Comm.*, **78**: 167-177 (1989).

28. Goddard, E.D., Matteson, G.H., and Totten, G.E., "Counterion Effects in a Cationic Monolayer", *Journal of Colloid and Interface Science*, **85:** (1982).

29. Groth, S., Steiff, A., and Weinspach P., "Influence of Drag Reducing Additives on the Measurement Accuracy of Heat Meters", Universität Dortmund, (1994).

30. Hammer, F., "Smooth Water for District Heating", *Fernwärme International*, **22**: 142-150 (1993).

31. Hammer, F., Personal communication, 1998.

32. Harwigsson, I., and Hellsten, M., "Environmentally Acceptable Drag-Reducing Surfactants for District Heating and Cooling", *JAOCS*, **73:** 921-928 (1996).

33. Hellsten, M., and Harwigsson I., "A New Biodegradable Friction Reducing Additive (FRA) for District Cooling Networks", *International District Energy Association Annual Conference Proceedings*, **85**: 282-299 (1994).

34. Hoffmann, H., Hofmann, S., Rauscher, A., and Kalus, J., "Shear Induced

Transitions in Micellar Solutions", *Progr. Colloid Polymer Sci*, **84**: 24-35 (1991).

35. Hoffmann, H., Rehage, H., Reizlein, K., and Thurn H., "Viscoelastic Detergent Solutions from Rodlike Micelles", in Shaw, D.O. (ed.) *ACS Symposium Series,* **272:** 41-66 (1985).

36. Hoyer, K., Bewersdorff, H.W., and Gyr, A., "A Study of Thread Riblets", *Applied Scientific Research*, **52**: 169-172 (1994).

37. Hoyer, K., and Gyr, "Turbulent Velocity Field in a Heterogeneously Drag Reduced Pipe Flow", *J. Non-Newtonian Fluid Mech.*, **65**: 221-240 (1996).

38. Hoyt, J.W., "The Effect of Additives on Fluid Friction", *Trans ASME, Journal of Basic Engineering*, **94**: 258-285 (1972).

39. Hu, Yuntao and Matthys, Eric F., "Characterization of Micellar Structure Dynamics for a Drag-Reducing Surfactant Solution Under Shear: Normal Stress Studies and Flow Geometry Effects", *Rheol. Acta*, **34**: 45-460 (1995).

40. Kostic, M., "On Turbulent Drag Reduction and Heat Transfer Reduction Phenomena and Laminar Heat Transfer Enhancement", *Int. J. Heat Mass Transfer*, **37:** 133-147 (1994).

41. Lu, B., Li, X., Zakin J.L., and Talmon, Y., "A Non-Viscoelastic Drag Reducing Cationic Surfactant System", *J. Non-Newtonian Fluid Mech.*, **71**: 59-72 (1997).

42. Matthys, E.F., "Heat Transfer, Drag Reduction and Fluid Characterization for Turbulent Flow of Polymer Solutions: Recent Results and Research Needs", *J. Non-Newtonian Fluid Mech.*, **38**: 313-342 (1991).

43. Matthys, E.F. and Sabersky, R.H., "A Method of Predicting the Diameter Effect for Heat Transfer and Friction of Drag Reducing Fluids", *Int. J. Heat Mass Transfer*, **25:** 1343-1351 (1982).

44. Mizushina, T, and Usui, H., "Reduction of Eddy Diffusion for Momentum and Heat in Viscoelastic Fluid Flow in a Circular Tube", *The Physics of Fluids*, **20**: S100-S108 (1977).

45. Myska, J., and Stern, P., "Properties of a Drag Reducing Micelle System", *Colloid and Polymer Sci.* **272:** 542-547 (1994).

46. Myska, J., and Simeckova, M., "The Shape of Micelles of a Complex Soap Causing the Toms Effect", *Colloid and Polymer Sci.*, **261:** 171-175 (1983).

47. Myska, J., and Zakin, J.L., "Differences in the Flow Behaviours of Polymeric and Cationic Drag Reducing Additives", *Ind. Eng. Chem. Res.* **36:** 5483-5487 (1997).

48. Myska, J., and Zakin, J.L., "Comparison of Flow Behaviours of Polymeric and Cationic Surfactant Drag Reducing Additives", *Proceedings of the 1996 ASME Fluids Engineering Division Summer Meeting*, San Diego, CA, 165-168 (1996).

49. Myska, J., Zakin, J.L. and Chara, Z., "Viscoelasticity of a Surfactant and Its Drag Reducing Ability", *Applied Scientific Research*, **55**: 297-310 (1996).

50. Ohlendorf, D., Interthal, W., and Hoffmann, H., "Surfactant Systems for Drag Reduction: Physical-Chemical Properties and Rheological Behaviour", *Rheologica Acta*, **25**: 468-486 (1986).

51. Patterson, G.K., and Florez, G.L., "Velocity Profiles During Drag Reduction", from *Viscous Drag Reduction*, Proceedings of the Symposium on viscous Drag Reduction held at the LTV Research Center, Dallas, Texas, Sept. 24-25, 1968, Plenum Press, NY, (1969).

52. Perry, R. and Green, G., Perry's Chemical Engineers' Handbook (1984).

53. Pollert, J., and Sellin, R.H.J., "Mechanical Degradation of Drag Reducing Polymer and Surfactant Additives: A Review", *Proc. of Int. Conf. Drag Reduction in Fluid Flow*, Ellis Horwood Ltd,.179-189 (1989).

54. Pollert, J., Komrzy, P., Srejkovsky, K., Pollert, J. (Jun.), Lu, B., and Zakin, J.L., "Drag Reduction and Heat Transfer of Cationic Surfactant Solutions", *Proceedings of the 1996 ASME Fluids Engineering Division Summer Meeting*, San Diego, CA, 31-36 (1996).

55. Radin, I., Zakin, J.L. and Patterson, G.K., "Exploratory Drag Reduction Studies in Non-Polar Soap Systems" from *Viscous Drag Reduction*, Proceedings of the Symposium on viscous Drag Reduction held at the LTV Research Center, Dallas, Texas, Sept. 24-25, 1968, Plenum Press, NY, 213-231 (1969).

56. Rehage, H., and Hoffmann, H., "Viscoelastic Detergent Solutions", *Faraday Discuss. Chem. Soc.*, **76**: 363-373 (1983).

57. Rehage, H., Wunderlich, I., and Hoffmann, H., "Shear Induced Phase Transitions in Dilute Aqueous Surfactant Solutions", *Progr Colloid & Polymer Sci.*, **72**: 51-59, (1986).

58. Renardy, M., "On the Mechanism of Drag Reduction", *J. Non-Newtonian Fluid Mech.*, **59**: 93-101, (1995).

59. Rose, G.D., Foster, K.L., "Drag Reduction and Rheological Properties of Cationic Viscoeleastic Surfactant Formulations", *Journal of Non-Newtonian Fluid Mechanics*, **31:** 59-85 (1989).

60. Rose, G.D., Foster, K.L., Slocum, V.L., and Lenhart, J.G., "Drag Reduction and Heat Transfer Characteristics of Viscoelastic Surfactant Formulations", *Proc. 3rd Int. Cong. On Drag Red'n*, Sellin, R.H.J., Moses, R.T., eds., U of Bristol, England, Paper D-6 (1984).

61. Savins, J.G., "A Stress-Controlled Drag-Reduction Phenomenon", *Rheologica Acta*, **6**: 323-330 (1967).

62. Savins, J.G., "Contrasts in the Solution Drag Reduction Characteristics of Polymeric Solutions and Micellar Structure", from *Viscous Drag Reduction, Proceedings of the Symposium on Viscous Drag Reduction,* held at the LTV Research Center, Dallas, Texas, Sept. 24-25, 1968, Plenum Press, NY, (1969).

63. Sellin, R., and Ollis, M., "Effect of Pipe Diameter on Polymer Drag Reduction", Ind. Eng. Chem. Prod. Res. Dev., **22**: 445-452 (1983).

64. Shaver, R.G., and Merrill, E.W., "Turbulent Flow of Pseudoplastic Polymer Solutions in Straight Cylindrical Tubes", *AIChE Journal*, **5:** 181-190 (1959).

65. Shenoy, A..V., "Drag Reduction with Surfactants at Elevated Temperatures", *Rheol. Acta*, **15**: 658-664 (1976).

66. Shenoy, A.V., "A Review on Drag Reduction with Special Reference to Micellar Systems", *Colloid & Polymer Sci.*, **282**: 319-337 (1984).

67. Schmitt, K., Durst, F., and Brunn, P., "Surfactant Additives in Pipe Flows Under Cyclic Heating Conditions", in Sellin, R.H. and Moses, R.T. (eds.) *Drag Reduction in Fluid Flows*, Ellis Horwood (1989).

68. Steiff, A., Althaus, W., Weber, M., and Weinspach, P., "Application of Drag Reducing Additives in District Heating Systems - Present State of Investigations" in Sellin, R.H. and Moses, R.T. (eds.) *Drag Reduction in Fluid Flows*, Ellis Horwood, 247-254 (1989).

69. Steiff, A., and Klopper, M., "Application of DRAs in District Heating Systems", *Proceedings of the 1996 ASME Fluids Engineering Division Summer Meeting*,

San Diego, CA, 235-242 (1996).

70. Toms, B.A., "Some Observations on the Flow of Linear Polymer Solutions Through Straight Tubes at Large Reynolds Numbers", *Proc. Ist Int. Congress on Rheology*, **2**:135-142 (1949).

71. Virk, P.S., "An Elastic Sublayer Model for Drag Reduction by Dilute Solutions of Linear Macromolecules", *J. of Fluid Mechanics*, **45**: 417-440 (1971).

72. Weinspach, P.-M., "Modelling of the Location and Requirements for Heat Exchangers in District Heating Networks using Friction Reducing Additives", *Advanced Energy Transmission Fluids for District Heating and Cooling, International Energy Agency Programme of Research, Development and Demonstration on District Heating and Cooling*, **N2:** (1996).

73. Young, John, Personal communication, 1995.

74. Young, John, Personal communication, 1999.

75. Young, John C. O'C., "Drag Reduction in the Chilled Water Distribution System of a 200-ton Absorption Chiller", *International District Energy Association Conference Proceedings*, **85**: 153-164 (1994).

76. Zakin, Jacques L. and Lui, Hsiao-Lung, "Variables Affecting Drag Reduction by Nonionic Surfactant Additives", *Chem. Eng. Commun.*, **23**: 77-88 (1993).

77. Zakin, J.L., Myska, J. and Chara, Z., "New Limiting Drag Reduction and Velocity Profile Asymptotes for Non-Polymeric Additive Systems", *AIChE Journal*, **42:** 3544-46 (1996).

APPENDIX A - SAMPLE CALCULATIONS

Sample Calculations

These calculations were carried out with data for the 40°C experimental run for FRA_1 with obstruction plate 2 at 3.65 m/s.

1. Correction of pressure data for blank obstruction plate with FRA_1 at 40°C and 3.65 m/s.

Pressure tap	Distance from junction (metres)	Cumulative pressure measurements (in. H_2O)	Line of best fit values (in. H_2O)	Offset values
1	0.0873	5.60	5.66	0.06
2	0.1746	6.78	6.90	0.12
3	0.2619	7.82	8.14	0.32
4	0.3492	9.82	9.39	-0.43
5	0.4366	10.69	10.63	-0.06
6	0.5239	12.18	11.88	-0.30
7	0.6112	12.77	13.12	0.35
8	0.7858	15.89	15.61	-0.28
9	1.0478	19.13	19.35	0.22

From linear regression, a line of best fit was developed for the pressure data in column 3 above as a function of distance. The equation of the line is y=14.253x+4.112.

'Offsets' were then developed for the data set, where the offset value=corrected value - measured value.

2. Applications of offsets to data for obstruction 2

The pressure data measurements were corrected by adding the offsets in column 5 above to the measured values (corrected value = measured value + offset).

Pressure tap	Distance from junction (metres)	Cumulative pressure measurements (in. H_2O)	Corrected pressure measurements (in. H_2O)	Differential pressure (in. H_2O)
1	0.0873	59.96	60.02	60.02
2	0.1746	61.83	61.95	1.93
3	0.2619	63.15	63.47	1.52
4	0.3492	65.25	64.82	1.34
5	0.4366	66.22	66.16	1.35
6	0.5239	67.64	67.34	1.17
7	0.6112	68.24	68.59	1.25
8	0.7858	71.31	71.03	2.44
9	1.0478	74.45	74.67	3.63

3. Differential pressures were calculated from the corrected pressure data (see column 5 above). Distances differentials were also calculated.

4. Calculation of Fanning friction factors over the distance intervals

The Fanning friction factor was calculated from:

$$f = \frac{D}{2\rho u^2}\frac{dP}{dL}$$

$$f = \frac{0.01705m}{2\times\left(991.83\frac{kg}{m^3}\right)\times\left(3.65\frac{m}{s}\right)^2}\frac{1.247\times 108\frac{N}{m^2}}{0.262m}$$

$$= 0.0023$$

At pressure tap 9, $\Delta P = 3.63$, and $\Delta L = 0.262$ m, f_9 is equal to 0.0043
At pressure tap 1, $\Delta P = 60.02$, and $\Delta L = 0.0873$ m, f_1 is equal to 0.0023

5. Following the same procedure, friction factors for water with obstruction 2 were calculated. For tap 1, $f_{water} = 0.1238$. For tap 9, $f_{water} = 0.0048$.

6. Percent friction reduction calculation

Percent friction reduction, or FRA effectiveness, was calculated from:

$$\eta = \frac{f_{solvent} - f_{fra}}{f_{solvent}} \times 100\%$$

η_1 =12.33

η_{10}= 51.27

APPENDIX B - ERROR CALCULATIONS

Error Calculations

1. Error inherent in friction factor calculations

Error assumptions

- The diameter of the Inconel tubing is accurate to within 1% (confirmed with vernier caliper measurements).
- Pressure transducer measurements were accurate to within 0.5% of the full range of the transducer (manufacturer's specifications).
- Because of temperature variations during the course of the experiment which varied by a maximum of 4°C during the course of any of the runs, density varied by 2.5 kg/m^3 (corresponding to a temperature change of 4°C).
- The flow rate varied by ±0.03 m3/h which corresponded to variations in velocity of ±0.03m/s. Two calculations are carried out below: one for the highest flowrate and one for the lowest flowrate.
- The location of the pressure taps was estimated to be accurate to within 1 mm. This would create a maximum error of 2 mm in the differential length. The minimum differential distance between taps (which would have created the maximum error) was 8.73 cm.

The Fanning friction factor is calculated from:

$$f = \frac{D}{2\rho u^2}\frac{dP}{dL}$$

$$= \frac{\left(D \pm \frac{1}{100}D\right)}{2\left(\rho \pm \frac{2.5}{980}\rho\right)\left(u \pm \frac{0.03}{3.65}u\right)^2}\frac{\left(dP \pm \frac{0.5}{100}\right)}{\left(dL \pm \frac{0.002}{0.0873}\right)}$$

$$= f \pm \sqrt{\left(\frac{1}{100}\right)^2 + \left(\frac{2.5}{980}\right)^2 + 2\left(\frac{0.03}{3.65}\right)^2 + \left(\frac{0.5}{100}\right)^2 + \left(\frac{0.002}{0.0873}\right)^2}\, f$$

$$= f \pm 2.8\%\, f$$

For the lowest flowrates of 2.0 m/s, the variability in the flow rate was smaller (±0.02 m/s). The corresponding error is ±2.9% f.

2. Error in friction reduction calculations

Percent friction reduction, or FRA effectiveness is calculated from:

$$\eta = \frac{f_{solvent} - f_{fra}}{f_{solvent}} \times 100\%$$

$$= \eta \pm \sqrt{3(0.02813)^2}\,\eta$$

$$= \eta \pm 4.9\%\,\eta$$

The corresponding error in percent friction reduction for the lowest flowrates is ± 5.0%η.

APPENDIX C - MATERIAL SAFETY DATA SHEETS FOR ETHOQUAD O/12 H AND ETHOQUAD O/12 PG

Akzo Nobel Chemicals Inc.
MATERIAL SAFETY DATA SHEET

DATE PRINTED: 11/16/1999 **PAGE 1**
MSDS NO. 15-074499

ETHOQUAD O/12PG

SECTION 1. CHEMICAL PRODUCT AND COMPANY INFORMATION

PRODUCT NAME
ETHOQUAD O/12PG

CHEMICAL NAME
N,N-bis(2-hydroxyethyl)-N-methyl-(Z)-9-octadecen-1-aminium chloride

SYNONYM
N,N-bis(2-hydroxyethyl)methyl octadecenyl ammonium chloride

CHEMICAL FORMULA
R-N(CH3)(CH2CH2OH)2Cl R=Oleyl

CAS #
18448-65-2

CHEMICAL FAMILY
Quaternary ammonium salt/glycol

MANUFACTURERS NAME
Akzo Nobel Chemicals Inc.

PRODUCT/TECHNICAL INFORMATION
1-800-906-9977

ADDRESS
300 South Riverside Plaza
Chicago, IL 60606

MEDICAL/HANDLING EMERGENCY
1-914-693-6946

COUNTRY
U.S.A.

TRANSPORTATION EMERGENCY
CHEMTREC 1-800-424-9300

PRODUCT USE
Surfactant

REVISION DATE
6/12/1998

ISSUE DATE
11/02/1994

REVISION NO.
003

SECTION 2. COMPOSITION/INFORMATION ON INGREDIENTS

SUBSTANCE DESCRIPTION	PERCENT	CAS#
N,N-Bis(2-hydroxyethyl)-N-methyl-9-octadecen-1-ammonium chlorides	74.000- 77.000	18448-65-2
1,2-Propanediol	22.000- 25.000	57-55-6
Bis(2-hydroxyethyl)-9-octadecene-1-amine	** 0.001- 2.000	25307-17-9
Bis(2-hydroxyethyl)-9-octadecenamine hydrochloride	0.001- 2.000	NOT ASSIGNE

** SUBSTANCE IS A COMPOUND AND/OR MIXTURE

SECTION 3. HAZARDS IDENTIFICATION

Appearance & Odor
Yellow liquid with a bland odor.

STATEMENT OF HAZARDS
DANGER
CAUSES SKIN AND EYE BURNS

Fire & Explosion Hazards
This product is not defined as flammable or combustible. However, under fire conditions it may support combustion and produce toxic oxides of carbon and nitrogen and hydrogen chloride. Under non-ideal oxidizing conditions, incomplete combustion may produce hydrogen cyanide.

Primary Route of Exposure
Skin and eye contact are the primary routes of exposure to this product.

SECTION 1. CHEMICAL PRODUCT AND COMPANY INFORMATION

PRODUCT NAME
ETHOQUAD O/12H

CHEMICAL NAME
N,N-Bis(2-hydroxyethyl)-N-methyl-(Z)-9-octadecen-1-aminium chloride

SYNONYM
N,N-Bis(2-hydroxyethyl)methyl octadecenyl ammonium chloride

CHEMICAL FORMULA
R-N(CH3)(CH2CH2OH)2Cl
R=Oleyl

CAS #
18448-65-2

CHEMICAL FAMILY
Quaternary ammonium salt/alcohol

MANUFACTURERS NAME
Akzo Nobel Chemicals Inc.

PRODUCT/TECHNICAL INFORMATION
1-800-906-9977

ADDRESS
300 South Riverside Plaza
Chicago, IL 60606

MEDICAL/HANDLING EMERGENCY
1-914-693-6946

COUNTRY
U.S.A.

TRANSPORTATION EMERGENCY
CHEMTREC 1-800-424-9300

PRODUCT USE
Surfactant

REVISION DATE
6/12/1998

ISSUE DATE
4/15/1994

REVISION NO.
004

SECTION 2. COMPOSITION/INFORMATION ON INGREDIENTS

SUBSTANCE DESCRIPTION	PERCENT	CAS#
N,N-Bis(2-hydroxyethyl)-N-methyl-9-octadecen-1-ammonium chlorides	74.000- 77.00C	18448-65-2
Isopropyl alcohol	22.000- 25.00C	67-63-0
Water	0.001- 3.00C	7732-18-5
Bis(2-hydroxyethyl)-9-octadecene-1-amine	** 0.001- 2.00C	25307-17-9
Bis(2-hydroxyethyl)-9-octadecenamine hydrochloride	0.001- 2.00C	NOT ASSIGNE

** SUBSTANCE IS A COMPOUND AND/OR MIXTURE

SECTION 3. HAZARDS IDENTIFICATION

Appearance & Odor
Yellow liquid with an isopropanol odor.

STATEMENT OF HAZARDS
DANGER
FLAMMABLE LIQUID AND VAPORS.
MAY CAUSE SKIN AND EYE BURNS AND RESPIRATORY TRACT IRRITATION.
OVEREXPOSURE MAY CAUSE HEADACHE, DIZZINESS AND NAUSEA
ALONG WITH DEFATTING OF THE SKIN WITH ITCHING AND
DERMATITIS IN SOME INDIVIDUALS.

Fire & Explosion Hazards
This product contains a volatile, flammable liquid and may produce flammable vapors. Vapors are heavier than air and may travel to a source of ignition and flash back. This product is sensitive to static discharge. Thermal decomposition products may include hydrogen chloride and toxic oxides of carbon and nitrogen. Under non-ideal oxidizing conditions, incomplete combustion may produce hydrogen cyanide.